PB-230 439

# THE EFFECT OF RAINFALL ON THE VELOCITY DISTRIBUTION IN SHALLOW CHANNEL FLOW

Larry Joe Glass

Texas A and M University

Prepared for:

Public Health Service

January 1965

DISTRIBUTED BY:

NTIS

National Technical Information Service
U. S. DEPARTMENT OF COMMERCE
5285 Port Royal Road, Springfield Va. 22151

PB 230 439

# THE EFFECT OF RAINFALL IN THE VELOCITY DISTRIBUTION IN SHALLOW CHANNEL FLOW

by

LARRY JOE GLASS

WATER RESOURCES INSTITUTE
TEXAS A&M UNIVERSITY
JANUARY 1965

THIS INVESTIGATION WAS SUPPORTED IN PART BY
PUBLIC HEALTH SERVICE RESEARCH GRANT WP00757-02
FROM THE DIVISION OF WATER SUPPLY AND POLLUTION CONTROL

Reproduced by
NATIONAL TECHNICAL
INFORMATION SERVICE
U S Department of Commerce
Springfield VA 22151

1.

100

TABLE OF CONTENTS


| Chapter | | Page |
|---|---|---|
| I. | INTRODUCTION | 1 |
| | REVIEW OF LITERATURE | 3 |
| | Velocity Distribution Studies | 3 |
| | Rainfall Simulators | 5 |
| II. | THEORETICAL DEVELOPMENT OF THE VELOCITY DISTRIBUTION EQUATION | 8 |
| III. | EQUIPMENT AND PROCEDURES | 17 |
| | Equipment | 17 |
| | Procedure | 26 |
| IV. | DATA ANALYSES AND DISCUSSION OF RESULTS | 30 |
| | Velocity Distribution Without Rainfall | 30 |
| | Velocity Distribution With Rainfall | 39 |
| | Shear at the Bed | 39 |
| | Resistance Coefficient | 45 |
| | Discussion of Variation in Results from the Theoretical | 48 |
| | Discussion of Variation Between Tests | 49 |
| | Nonuniform Flow | 49 |
| | Infinitely Wide Channel | 50 |
| | Instrumentation Error | 50 |
| | Statistical Analysis of the Data | 52 |
| V. | SUMMARY AND CONCLUSIONS | 54 |
| BIBLIOGRAPHY | | 56 |
| APPENDIX | | 58 |
| | List of Symbols | 59 |


Pages ii and iii are Blank.

LIST OF TABLES


| Table | | Page |
|---|---|---|
| I. | Regression Analysis Results of Equation 22 for Tests Conducted Without Simulated Rainfall. . . . . | 38 |
| II. | Regression Analysis Results of Equation 22 for Tests Conducted With Simulated Rainfall . . . . . | 40 |
| III. | Regression Analysis Results of Equation 23 for Tests Conducted Without Simulated Rainfall. . . . . | 46 |
| IV. | Regression Analysis Results of Equation 23 for Tests Conducted With Simulated Rainfall . . . . . | 47 |
| V. | Summary of Analysis of Variance Tests Between Variables Compared. . . . . | 53 |
| VI. | Hydraulic Flume Data and Velocity Distribution Calculations Using the Prandtl Tube Without Simulated Rainfall on a Concrete Bed. . . . . | 61 |
| VII. | Hydraulic Flume Data and Velocity Distribution Calculations Using the Prandtl Tube With Simulated Rainfall on a Concrete Bed. . . . . | 66 |
| VIII. | Hydraulic Flume Data and Velocity Distribution Calculations Using the Total Head Probe Without Simulated Rainfall on a Concrete Bed. . . . . | 71 |
| IX. | Hydraulic Flume Data and Velocity Distribution Calculations Using the Total Head Probe With Simulated Rainfall on a Concrete Bed. . . . . | 73 |
| X. | Hydraulic Flume Data and Velocity Distribution Calculations Using the Prandtl Tube Without Simulated Rainfall on a Plywood Bed . . . . . | 75 |
| XI. | Hydraulic Flume Data and Velocity Distribution Calculations Using the Prandtl Tube With Simulated Rainfall on a Plywood Bed . . . . . | 77 |

Table

Page

XII. Hydraulic Flume Data and Velocity Distribution Calculations Using the Pitot-Static Tube Without Simulated Rainfall on a Plywood Bed. . . . . 79

XIII. Hydraulic Flume Data and Velocity Distribution Calculations Using the Pitot-Static Tube With Simulated Rainfall on a Plywood Bed. . . . . 81

XIV. Hydraulic Flume Data and Velocity Distribution Calculations Obtained from Smerdon's Doctoral Dissertation Using a Darcy Tube. Tests Run Over Several Missouri Soils . . . . . 83

XV. Analysis of Variance Results Comparing Rainfall and No Rainfall for the Prandtl Velocity Sensing Probe and Concrete Bed Data. . . . . 87

XVI. Analysis of Variance Results Comparing Rainfall Using a Total Head Velocity Sensing Probe and Concrete Bed Data. . . 87

XVII. Analysis of Variance Results Comparing Rainfall and No Rainfall for the Prandtl Velocity Sensing Probe and Plywood Bed Data. . . . . 88

XVIII. Analysis of Variance Results Comparing Rainfall and No Rainfall for the Pitot-Static Velocity Sensing Probe and Plywood Bed Data . . . . . 88

XIX. Analysis of Variance Results Comparing Bed Data for the Prandtl Velocity Sensing Probe Without Rainfall. . . . . 89

XX. Analysis of Variance Results Comparing Bed Data for the Prandtl Velocity Sensing Probe With Rainfall . . . . . 89

XXI. Analysis of Variance Results Comparing the Prandtl and the Total Head Velocity Sensing Probes for the Concrete Bed Data Without Rainfall. . . . . 90

XXII. Analysis of Variance Results Comparing the Prandtl and the Pitot-Static Velocity Sensing Probes for the Plywood Bed Data Without Rainfall . . . . . 90

Table

Page

XXIII. Analysis of Variance Results Comparing a Darcy and the Prandtl Velocity Sensing Probes for the Soil Bed and a Concrete Bed Data Without Rainfall. . . . . 91

XXIV. Analysis of Variance Table Comparing a Darcy and the Prandtl Velocity Sensing Probes for the Soil Bed and a Plywood Bed Data Without Rainfall . . . . . 91

XXV. Group Totals Used in Statistical Analysis of Variance. . . . 92

## LIST OF FIGURES


| Figure | | Page |
|---|---|---|
| 1. | Sketch of Theoretical Velocity Distribution Near a Smooth Boundary. . . . . | 10 |
| 2. | Sketch of Theoretical Velocity Distribution Near a Rough Boundary . . . . . | 10 |
| 3. | Overall View of Research Flume and Rainfall Simulator. . . . . | 18 |
| 4. | Inlet Section of the Hydraulic Flume . . . . . | 18 |
| 5. | Manometer Board Indicating Slope of Water Surface and Depths of Flow Along the Flume . . . . . | 20 |
| 6. | H-type Flow Rate Measuring Flume and Water Level Recorder . . . . . | 20 |
| 7. | Three Pumps and Water Supply Sump. Small Pump Provided Water Supply for Rainfall Simulator. . . . . | 21 |
| 8. | Schematic of Facilities Used for this Study. . . . . | 23 |
| 9. | Flow in Research Flume With Simulated Rainfall . . . . . | 24 |
| 10. | Flow in Research Flume Without Simulated Rainfall. . . . | 24 |
| 11. | Traversing Mechanism and Prandtl Tube Positioned in the Research Flume. . . . . | 25 |
| 12. | Inclined Water-to-Air Manometer to Measure the Point Velocities Within the Flow . . . . . | 25 |
| 13. | The Three Velocity Sensing Probes: Pitot-static Tube, Prandtl Tube, and the Total Head Tube. . . . . | 27 |
| 14. | Rainfall Pattern and Resulting Cross-sectional Velocity Distribution for 0.3 Feet Depth of Flow. . . . . | 31 |

| Figure | | Page |
|---|---|---|
| 15. | Cross-Sectional Velocity Distribution for 0.3 Feet Depth of Flow Without Simulated Rainfall . . . . . | 31 |
| 16. | Velocity Distribution Regression Curve Using the Prandtl Tube Without Simulated Rainfall on a Concrete Bed. . . . . | 33 |
| 17. | Velocity Distribution Regression Curve Using the Total Head Tube Without Simulated Rainfall on a Concrete Bed. . . . . | 34 |
| 18. | Velocity Distribution Regression Curve Using the Prandtl Tube Without Simulated Rainfall on a Plywood Bed . . . . . | 35 |
| 19. | Velocity Distribution Regression Curve Using the Pitot-static Tube Without Simulated Rainfall on a Plywood Bed. . . . . | 36 |
| 20. | Velocity Distribution Regression Curve from Smerdon Data Using a Darcy Tube Without Simulated Rainfall on a Soil Bed. . . . . | 37 |
| 21. | Velocity Distribution Regression Curve Using the Prandtl Tube With Simulated Rainfall on a Concrete Bed. . . . . | 41 |
| 22. | Velocity Distribution Regression Curve Using the Total Head Tube With Simulated Rainfall on a Concrete Bed. . . . . | 42 |
| 23. | Velocity Distribution Regression Curve Using the Prandtl Tube With Simulated Rainfall on a Plywood Bed. . . . . | 43 |
| 24. | Velocity Distribution Regression Curve Using the Pitot-static Tube With Simulated Rainfall on a Plywood Bed. . . . . | 44 |

# CHAPTER I

## INTRODUCTION

Velocity distribution in pipes and open channels has been the subject of considerable research. However, no studies have been made to determine the effect of rainfall on the velocity distribution in shallow channel flow.

Vanoni (14) has shown in his studies of sediment transport in streams that the suspended sediment concentration depends on the vertical velocity distribution in the flow. Because soil erosion occurs during rainfall, most of the shallow flowing streams will be transporting sediment toward the larger streams during the rainfall period. The effect of the rainfall on the velocity distribution, and thus the suspended sediment transport capacity of the shallow stream, is unknown.

Studies to determine the effect of rainfall on the velocity distribution are needed to better predict the suspended sediment transport capacity of shallow streams. According to Bennett (1), tens of millions of dollars are required each year for repairing damages and providing maintenance on water utilization facilities, such as reservoirs and rivers, because of sediment in the streams. Brown (3) states that surveys from five per cent of the 10,000 existing reservoirs in the United States, show their aggregate capacity is being reduced by more than 350,000 acre-feet annually. This is equivalent

to the volume of a reservoir large enough to provide water for one year to a city of 250,000 population or irrigate an area of 100,000 acres.

A better understanding of the mechanics of sediment transport during the duration of the rainfall will aid in developing ways of reducing the sediment load in our streams. The need for clean water in our streams and rivers is increasing the demand for more water for domestic purposes. Brown (2) has stated that

> ...as a result of silting alone 21 per cent of the Nation's water supply reservoirs will have a useful life of less than 50 years, another 25 per cent will last 50 to 100 years, whereas only 54 per cent provide enough storage to suffice for present requirements (not the estimated future needs) 100 years hence.

Our exploding population points to the need of better management of our sediment problems in streams. A thorough knowledge of how sediment is transported in the streams, and the effect rainfall has on the transporting characteristics is essential.

The objectives of this study were:

1. To determine the velocity distribution in shallow channel flow as affected by rainfall.
2. To compare measured velocity distributions, with and without rainfall, with theoretical distributions for turbulent flow.
3. To develop a relationship between the rainfall energy on shallow channel flow and the resultant shear forces at the bed of the channel.

# REVIEW OF LITERATURE

Very little literature is available concerning the effect of simulated rainfall on the velocity distribution in shallow channel flow. No known research has been directed specifically at this problem. However, the literature concerning velocity distribution in open channels has been reviewed in order to correlate the velocity distribution results obtained with simulated rainfall with those obtained without simulated rainfall.

Velocity distribution theories. Velocity distribution was studied as early as the seventeenth century when Galileo presented the fallacy of the "scala", which stated that the horizontal velocity in a stream increased with the depth in exactly the same manner as the vertical velocity of a falling body increased from its original position (6). It was not until 1812, a century and a half later, when Woltman inverted the velocity distribution diagram introduced by Galileo, that the concept presented began to develop into the present theory. Since that time numerous analyses of the vertical velocity distribution have been made.

The introduction of the mixing length theory by Prandtl in 1925 marked the beginning of great progress in the theoretical analysis of turbulent flow (10). Nikuradse and von Karman developed velocity distribution equations for pipes utilizing the mixing length theory (9). Wang examined the Prandtl and the von Karman formulas for velocity distribution and derived a new formula for the velocity distribution in

pipes (15). The new formula contained additional terms which appeared only to make the formula more cumbersome to use. Schlicting showed that the velocity distribution in a rectangular channel could be obtained using Prandtl's mixing length theory (10). Vanoni, using the von Karman universal logarithmic velocity distribution law for pipes, gave the following equation for uniform two-dimensional open channel flow

$$\frac{v - v_{max}}{\sqrt{gdS}} \quad \frac{2.3}{K} \log_{10} \frac{y}{d}$$

in which v is the velocity at any distance, y, above the channel bed, $v_{max}$ is the maximum velocity, g is the acceleration of gravity, d is the depth of flow, S is the slope of the channel, and $K$ (kappa) is von Karman's universal constant having a value of 0.4 for clear water flow in pipes (13).

The above equation is valid only for logarithmic velocity distributions. However, Vanoni stated that the striking similarity between observed distributions and those following the logarithmic law offer reasonable justification of the use of the law in calculating some of the performance characteristics of natural streams. Chow (4) indicates that channel roughness will change the vertical velocity distribution curve, but does not discuss this in terms of the logarithmic distribution.

Keulegan (5) states that for open channels the turbulent fluctuations near the surface are only two-dimensional, and are a source of energy dissipation because the velocity at the surface is not uniform. Studies determining the effect of rainfall on suppressing the region of maximum

horizontal velocity because of energy dissipation by the rain at the water surface have not been made.

Smerdon (11), in his study of the effect of rainfall on critical tractive forces in shallow channel flow, showed that the velocity distribution curves indicated lower velocities near the surface with rainfall than with no rainfall. Vertical velocity distribution at the center of the flume appeared to satisfy the logarithmic law of velocity distribution. Smerdon further found that the mean velocity of the flow was reduced with rainfall, and developed the following empirical logarithmic regression equation from flume data:

$$\frac{V}{V_R} = 0.958D^{-0.046}$$

where V is the mean velocity of flow without rainfall in feet per second, $V_R$ is the mean velocity of flow with rainfall in feet per second, and D is the depth of flow without rainfall in feet. In his study the depths of flow were always less than 0.4 feet. No reports on the effect of rainfall on vertical velocity distribution in shallow flow other than Smerdon's preliminary study can be found.

Rainfall simulators. Simulated rainfall should duplicate, as near as possible, the characteristics of natural rainfall if the results of simulated rainfall studies are to be related to field conditions. Some of the early studies with simulated rainfall were an attempt to duplicate natural rainfall energies for various rainfall in-

tensities.

Rainfall simulators have primarily been developed to accelerate erosion studies. Rainfall simulators are not a recent development. Lowdermilk, Duley and Hayes, Nichols and Sexton, and Hendrickson were among the first to make studies using simulated rainfall in the early 1930's (7). Types of rainfall simulators varied. Meyer (7) made an extensive review of all previous rainfall simulators with the purpose of defining the state of rainfall simulator development, and to incorporate all the desirable features in a portable erosion plot simulator. From his review, the following features were desired in a rainfall simulator:

1. A drop size distribution similar to that of natural rainfall.
2. Drop velocities of fall near terminal velocity of drops.
3. Intensities corresponding to the range of storms producing medium to high rates of runoff and erosion.
4. Satisfactory intensity and random drop size distribution over the area covered.
5. Minimum wind distortion.
6. Small effective area per nozzle, with resultant greater degree of uniformity.
7. Ability to reproduce a given storm.

Meyer then performed numerous tests with various commercial nozzles. He selected Spraying Systems Company Veejet and Fulljet nozzles as best meeting the requirements. Tests were also made to determine

velocity, drop size distribution, and kinetic energy. From extensive tests, Spraying Systems Company Veejet 80100 nozzles at a height of 8 feet operating with a nozzle pressure of 6 pounds per square inch were recommended. The distance between nozzles parallel to the long dimension of the spray pattern was 5 feet. This design was used for the rainfall simulator in this study.

# CHAPTER II

## THEORETICAL DEVELOPMENT OF THE VELOCITY DISTRIBUTION EQUATION

Velocity distribution is affected by the shear occurring between the boundary and the moving fluid. For laminar flow, the intensity of the shear may be defined as

$$\tau = \mu \, dv/dy \tag{1a}$$

in which $\tau$ (tau) is the intensity of shear, $\mu$ (mu) is the dynamic viscosity, and dv/dy is the velocity gradient at the boundary. However, for turbulent flow, the velocity fluctuates about a temporal mean value, $\bar{v}$, caused by the intermixing of the flow. The shear at a channel bed for turbulent flow is then expressed by

$$\bar{\tau} = \eta \, d\bar{v}/dy \tag{1b}$$

where $\bar{\tau}$ denotes the temporal mean shear intensity and $\eta$ (eta) is the eddy viscosity analogous to the dynamic viscosity in laminar flow. Dividing the eddy viscosity by the mass density, $\rho$ (rho), the kinematic eddy viscosity, $\epsilon$ (epsilon), is defined.

This parameter, $\epsilon$ , is dependent on the eddy velocity, $\sqrt{\bar{v}_1^2}$ , and the eddy size, l. The eddy size is often referred to as the mixing length. The eddy viscosity does not remain constant, but in pipe flow approaches a maximum approximately midway between the wall and

the center of the pipe. However, experiments indicate that the intensity of shear and the eddy viscosity vary in such a manner that their ratio approximates a direct proportion to $\sqrt{\tau_o/\rho}$, where $\tau_o$ is the boundary shear. This term is known as the shear velocity. Rewriting equation 1b and omitting the designation of temporal mean values

$$\frac{dv}{dy} = \frac{\tau}{\eta} = \frac{1}{y\,K}\sqrt{\tau_o/\rho} \tag{2}$$

in which y is the distance from the boundary and $K$ is the von Karman universal constant having a value of 0.4 for clear water flow in pipes. Integrating the preceding equation and eliminating $K$

$$v = 2.5\sqrt{\tau_o/\rho}\,\log_e y + C_1 \tag{3}$$

which $C_1$ is a constant of integration that must satisfy the boundary conditions. Letting y' be the value of y at which the logarithmic curve intersects the axis, i.e., where v = 0, equation 3 becomes

$$v = 2.5\sqrt{\tau_o/\rho}\,\log_e (y/y') \tag{4}$$

For smooth boundaries, the thickness of the laminar sublayer must be evaluated. A sketch of the sublayer and turbulent flow above this layer is shown in Figure 1. Define the distance from the boundary to the zone differentiating between laminar and turbulent flow to be $y = \delta$ (delta). Rouse (9) shows that this distance may be represented by a constant value of the stability parameter $\chi$ (chi) defined as

$$\chi = \frac{y^2\,dv/dy}{\nu} \tag{5a}$$

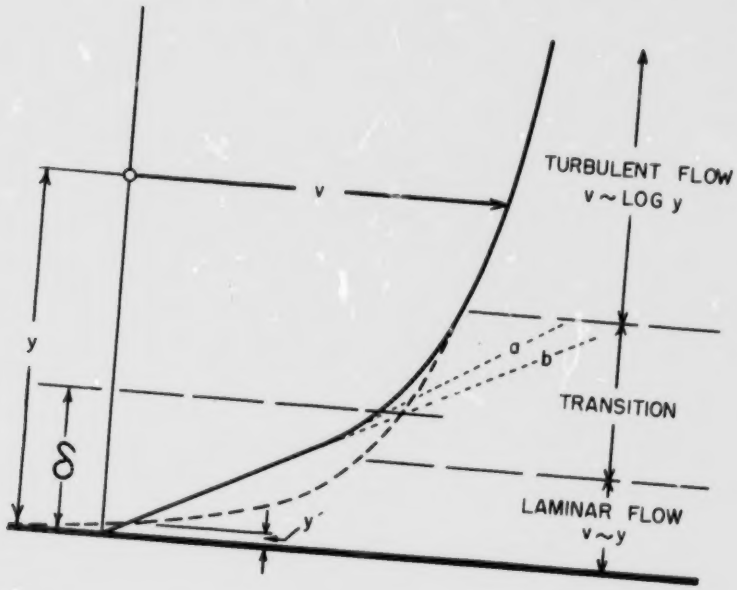


FIGURE 1. SKETCH OF THEORETICAL VELOCITY DISTRIBUTION NEAR A SMOOTH BOUNDARY

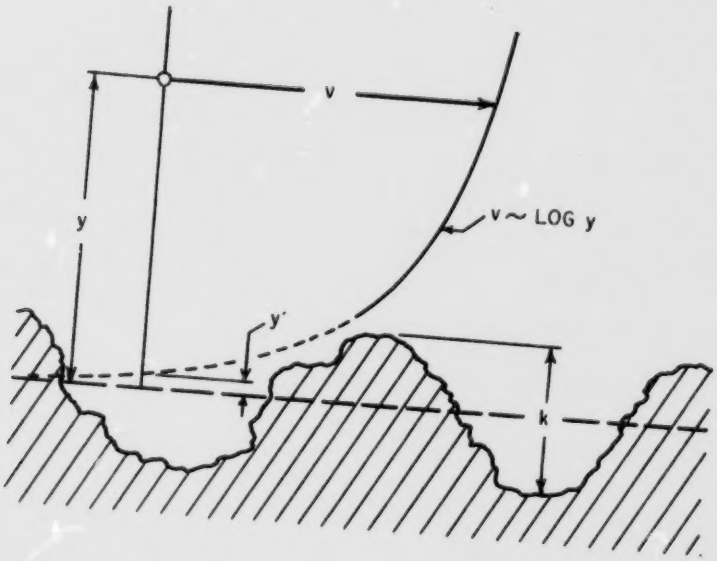


FIGURE 2. SKETCH OF THEORETICAL VELOCITY DISTRIBUTION NEAR A ROUGH BOUNDARY

in which $\nu$(nu) is the kinematic viscosity defined as $\mu/\rho$ . Substituting $y = \delta$ and letting the boundary shear be $\tau_o = \mu\, dv/dy$, the constant value of the stability parameter, $C_2$, may be expressed as

$$C_2 = \frac{\delta^2 \tau_o}{\mu \nu} \tag{5b}$$

Rearranging and letting B be another constant

$$\delta = \frac{\sqrt{C_2}\ \nu}{\sqrt{\tau_o/\rho}} = By' \tag{6}$$

Experimental studies by Nikuradse (9) on closed conduits showed that

$$\frac{v}{\sqrt{\tau_o/\rho}} = \sqrt{\tau_o/\rho}\ \frac{y}{\nu} = 11.6 \tag{7}$$

at the intersection of the laminar sublayer and the turbulent region. Again substituting $\delta$ for y, the distance from the boundary to the intersection of the laminar sublayer and the turbulent region can be expressed as

$$\delta = 11.6\, \frac{\nu}{\sqrt{\tau_o/\rho}} \tag{8}$$

Comparing equation 6 and equation 8, $\sqrt{C_2}$ must be 11.6. The constant, B, has been found by Nikuradse (9) to equal 107. Therefore, using equation 6 and 8

$$y' = \frac{\delta}{107} = \frac{11.6\ \nu}{107\sqrt{\tau_o/\rho}} = \frac{0.108\ \nu}{\sqrt{\tau_o/\rho}}$$

Substituting this value of y' into equation 4

$$\frac{v}{\sqrt{\tau_o/\rho}} = 2.5 \log_e \frac{y\sqrt{\tau_o/\rho}}{0.108}$$

or expressed in terms of common logarithms and simplified

$$\frac{v}{\sqrt{\tau_o/\rho}} = 5.75 \log_{10} \frac{y\sqrt{\tau_o/\rho}}{\nu} + 5.5 \qquad (9)$$

This equation is the Karman-Prandtl equation for the velocity distribution in turbulent flow near smooth boundaries.

For rough boundaries, a laminar sublayer is assumed not to exist when the roughness of the boundary, k, has a greater value than $\delta$ (Figure 2). Tests by Nikuradse (9), with sand grains of diameter k cemented to pipe walls, indicated for $k > 10\,\delta$

$$y' = \frac{k}{30} \qquad (10)$$

Assuming this to be the criteria for rough boundaries and substituting into equation 4 yields

$$\frac{v}{\sqrt{\tau_o/\rho}} = 2.5 \log_e \frac{30\,y}{k}$$

or

$$\frac{v}{\sqrt{\tau_o/\rho}} = 5.75 \log_{10} \frac{y}{k} + 8.5 \qquad (11)$$

which is the Karman-Prandtl equation for the velocity distribution in turbulent flow near rough boundaries.

Assuming the verification by Nikuradse of the theoretical equations for velocity distribution in pipes are valid for flow near boundaries in open channels, similar equations may be developed using

the mean velocity of the flow. Considering a unit width of flow, the flow in a rectangular channel is

$$q = \frac{Q}{b} = \int_0^d v\,dy \tag{12}$$

in which q is the unit discharge, Q is the total discharge, b is the width of the channel, and d is the total depth of flow.

For rough boundaries, equation 12 becomes

$$q = \int_0^d \left[5.75\sqrt{gdS}\ \log_{10}\frac{y}{k} + 8.5\sqrt{gdS}\right] dy$$

where $\sqrt{gdS}$ equals $\sqrt{\tau_o/\rho}$ for infinitely wide channels. S is the slope of the energy gradient and g is the gravitational acceleration. In terms of natural logarithms

$$q = \int_0^d \sqrt{gdS}\left[2.5\ \log_e\frac{y}{k} + 8.5\right] dy$$

and

$$Vd = 2.5\sqrt{gdS}\int_0^d \log_e\frac{y}{k}\,dy + 8.5\sqrt{gdS}\int_0^d dy$$

$$= \sqrt{gdS}\left[2.5d\ (\log_e\frac{d}{k} - 1) + 8.5d\right]$$

Dividing by the total depth, d, and converting back to common logarithms, the mean velocity, V, is

$$V = \sqrt{gdS}\left[5.75\ \log_{10}\frac{d}{k} + 6.0\right] \tag{13}$$

Subtracting equation 13 from equation 11

$$\frac{v - V}{\sqrt{gdS}} = 5.75\ \log_{10}\frac{y}{d} + 2.5 \tag{14}$$

Equation 14 is the general equation for the velocity distribution in infinitely wide open channels near smooth or rough boundaries. The derivation for the equation for smooth boundaries has been omitted since the result is identical.

Rouse (9) shows that the intensity of shear, $\tau_o$, which is included in the velocity distribution equation, is reduced as the distance from the boundary is increased. An expression for $\tau_o$ is

$$\frac{2C_3}{5\sqrt{xv_o/\nu}} \frac{\rho v_o^2}{2} \tag{15}$$

where $C_3$ is a constant, x is the distance along the boundary, and $v_o$ is the velocity at the nominal limit of the boundary layer. Substituting the surface drag coefficient, $C_f$, for $2C_3/5$ divided by the square root of the Reynolds number, $\sqrt{xv_o/\nu}$, gives

$$\tau_o = C_f \frac{\rho v_o^2}{2}$$

Replacing $v_o$ with the mean velocity, V, and introducing the relationship between the surface drag coefficient, $C_f$, and the Darcy-Weisbach resistance coefficient, f, which is $C_f = f/4$, gives

$$\tau_o = \frac{f \rho V^2}{8} \tag{16}$$

For uniform flow in open channels, the boundary shear is in equilibrium with the energy gradient. The product of the intensity of shear and boundary area per unit width should equal the product of the weight of the fluid on the unit area and the change in elevation per unit of dis-

tance, yielding

$$\tau_o = \gamma Sd \tag{17}$$

in which $\gamma$ (gamma) is the specific weight and S is the slope of the energy gradient. Combining equations 16 and 17 gives

$$\gamma Sd = \frac{f \rho V^2}{8} \tag{18}$$

Rearranging and introducing $g = \gamma/\rho$ yields

$$f = \frac{8\, g\, d\, S}{V^2} \tag{19}$$

Finally, introducing equation 19 into equation 14 gives another form of the dimensionless velocity distribution equation

$$\frac{v - V}{V\sqrt{f/8}} = 5.75 \log_{10} \frac{y}{d} + 2.5 \tag{20}$$

Rearranging

$$\frac{\frac{v}{V} - 1}{\sqrt{f}} = 2.03 \log_{10} \frac{y}{d} + 0.88 \tag{21}$$

A plot of equation 21 will give a general velocity distribution for an infinitely wide open channel.

Regression equations of velocity distributions obtained from this study are compared with the theoretical equations developed for rectangular open channel flow. The data are expressed in dimensionless terms with $\frac{v - V}{\sqrt{gdS}}$ and $\frac{y}{d}$ being the variables. Therefore, the analysis

is of the form of equation 14 and the results can easily be compared with the theoretical equation. The effect of rainfall upon the flow is also included in the analysis.

# CHAPTER III

## EQUIPMENT AND PROCEDURES

This study was conducted in the Soil and Water Research Laboratory of the Agricultural Engineering Department. The equipment used in this study will be given first followed by the procedures used in obtaining the data.

### Equipment

A rectangular research flume 72 feet long, 2.5 feet wide, and 1.33 feet deep was used for this study (Figure 3). The flume frame was supported on a single span truss with the lower-end supported on a pivot allowing the upper-end to be lifted with a pair of hydraulic jacks. This permitted any desired slope to a maximum of 1.5 per cent to be obtained. The sides and bottom of the flume were constructed of 3/4-inch marine plywood with a 1/32-inch plastic veneer on both sides.

A 2 x 2.5-foot three-sided box made of 3/4-inch marine plywood attached to the upper end of the flume provided the water entrance to the flume. A 6-inch accordion-type wire-reinforced rubber tubing was used to connect the pipeline to the box entrance. Figure 4 shows the water entrance. Baffles placed at the upper end of the flume dissipated much of the turbulence and reduced the surface roughness of the flow. The flume had clear plexiglas sides at a distance of 24 to 48 feet from the upstream end which permitted visual observation of the

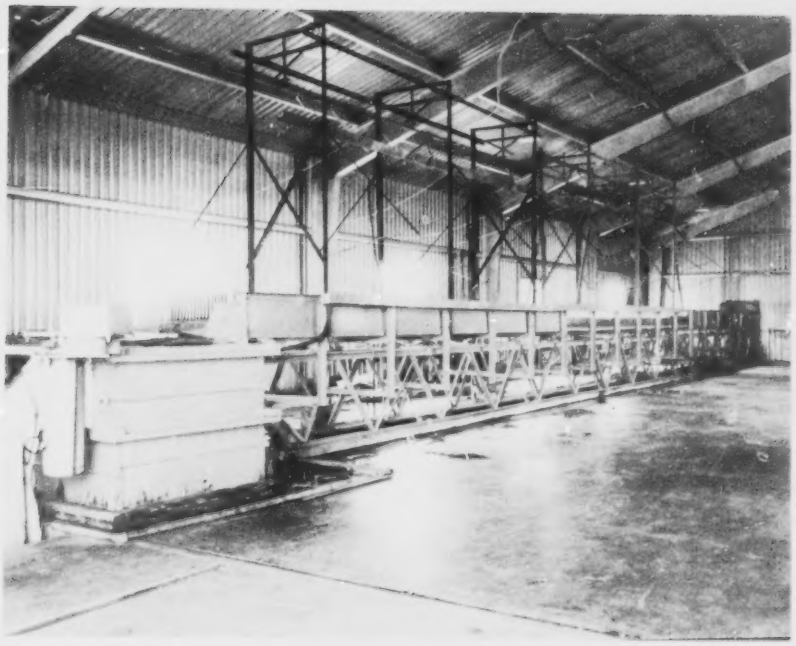

FIGURE 3. OVERALL VIEW OF RESEARCH FLUME AND RAINFALL SIMULATOR

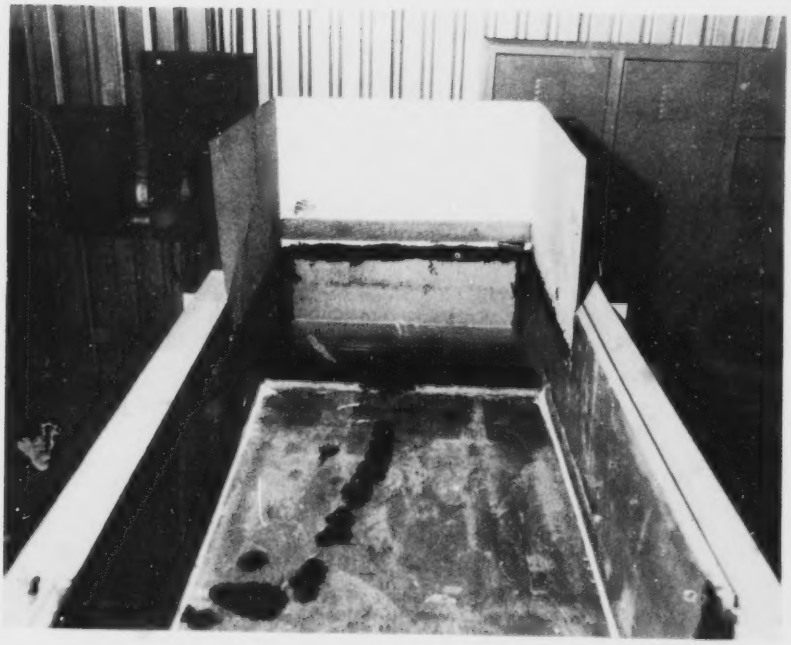

FIGURE 4. INLET SECTION OF THE HYDRAULIC FLUME

flow. Concrete slabs having a thickness of 2.5 inches were placed in the bottom of the flume for one series of tests. The concrete was roughened to simulate the roughness of a natural earth channel bed. The concrete slabs were removed and the marine plywood bottom was used for another part of the study. Seventeen piezometer orifices were spaced along the length of the flume and connected with transparent Tygon tubing to a central manometer board (Figure 5). The first piezometer orifice was located 4.0 feet from the upstream end of the flume. The first four orifices were spaced 6.0 feet apart, followed by ten orifices spaced 3.0 feet apart, and the remaining three spaced 6.0 feet apart.

A gate constructed of vertical slats was located at the outlet in the flume to maintain approximately uniform flow. Flow from the flume discharged into a tank 8.25 feet wide, 4.25 feet long and 3.5 feet deep. Discharge from this tank was through a 1.5-foot H-type flow rate measuring flume into a 25,000 gallon sump. The H-type flume was used for the flow measurements. The discharge was obtained from calibration tables. The depth of flow through the H-type flume was measured very accurately with a water level recorder and was used to determine the flow rates of this study. The tank, H-type flume, and water level recorder are shown in Figure 6.

The water supply was obtained from a 25,000-gallon sump from which water was pumped through a 6-inch pipe to the upstream end of the flume (Figure 7). Flow in the pipeline could be measured with a calibrated

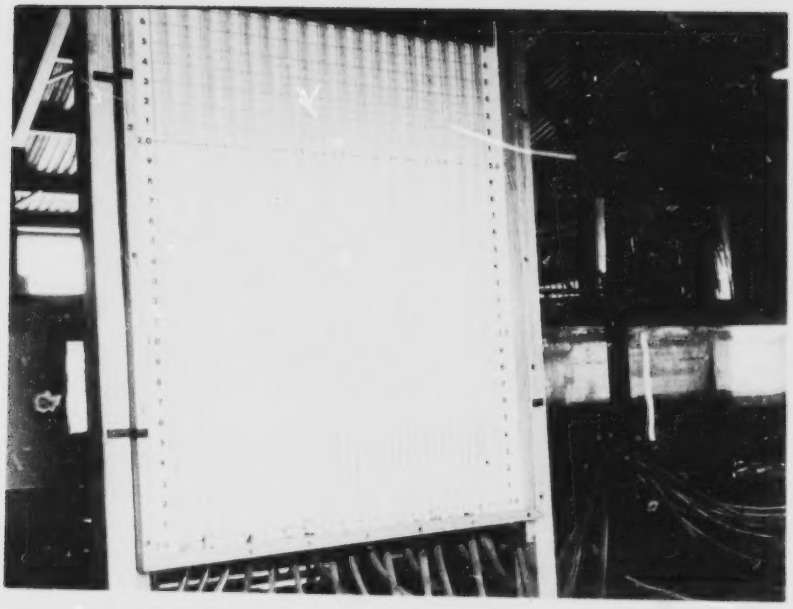

FIGURE 5. MANOMETER BOARD INDICATING SLOPE OF WATER SURFACE AND DEPTHS OF FLOW ALONG THE FLUME

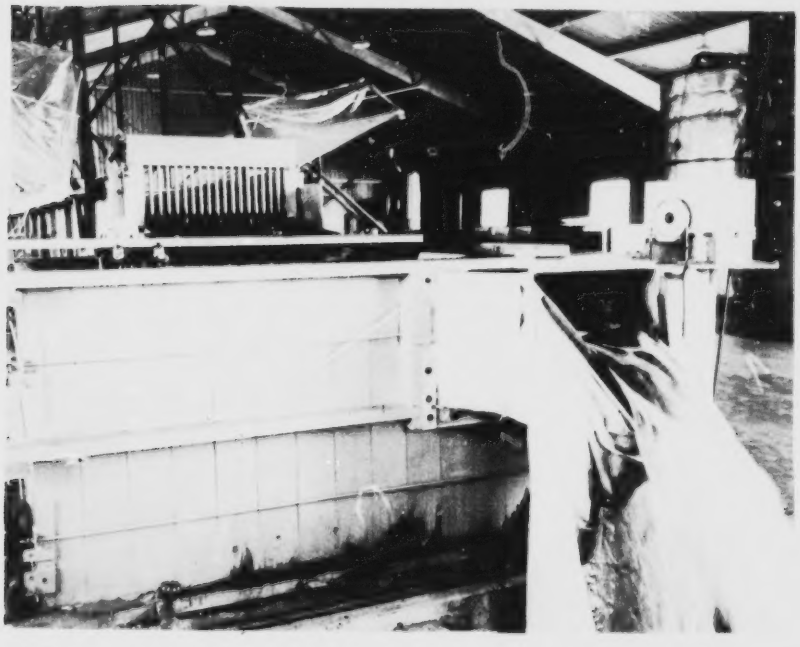

FIGURE 6 H-TYPE FLOW RATE MEASURING FLUME AND WATER LEVEL RECORDER

FIGURE 7 THREE PUMPS AND WATER SUPPLY SUMP. SMALL PUMP PROVIDED WATER SUPPLY FOR RAINFALL SIMULATOR

Dall-type flow nozzle. A well-type manometer having a scale range of 100 inches was connected to the Dall tube to measure the pressure differential. The indicating fluid in the manometer had a specific gravity of 2.95. A gate valve in the pipeline near the upstream end of the flume was used to regulate the flow rate into the flume. A schematic plan view of the flow system is shown in Figure 8.

The simulated rainfall for the study was produced from eight Spraying Systems Company 80100 Veejet nozzles located 5 feet apart. The nozzles were attached to a 1-inch pipe placed above the flume so the longitudinal axis of the pipe was directly above the longitudinal axis of the flume. The pipe was supported so that the distance from the nozzle tips to the flume bed was 8 feet. The framework for the rainfall simulator was mounted atop the research flume. The pressure for the simulator was controlled using a separate pump from that supplying the flume flow. The water was delivered to the nozzles through three 1-inch rubber hoses attached at each end and the middle of the simulator to provide a more uniform discharge from the nozzles. The water pressure at the nozzles was 6.0 pounds per square inch producing 4.0 gallons per minute from each nozzle. Figures 9 and 10 show the rainfall simulator with and without simulated rainfall.

The point velocities were measured with a Prandtl tube having a velocity coefficient of 1.0. The Prandtl tube was mounted on a track placed perpendicular to the flow in the flume (Figure 11). The support for the tube was constructed so that it could be moved in the

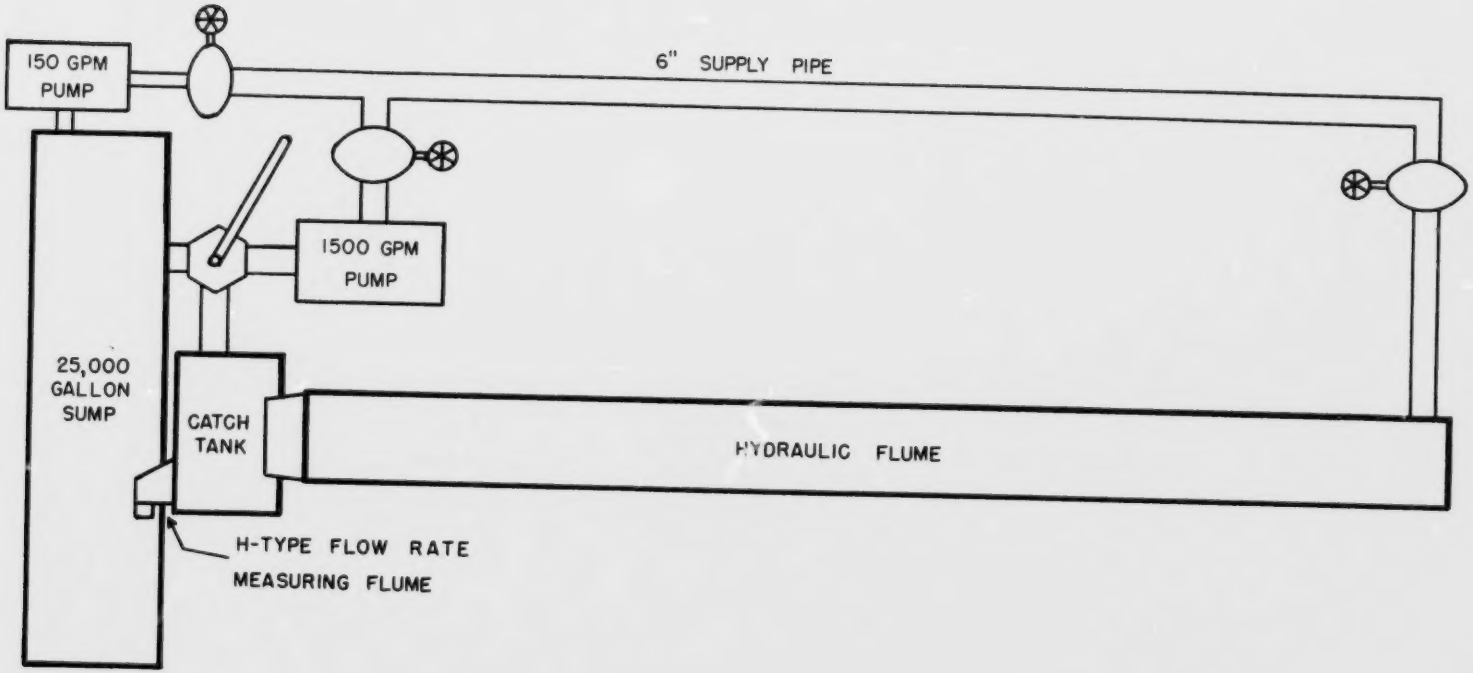


FIGURE 8. SCHEMATIC OF FACILITIES USED FOR THIS STUDY

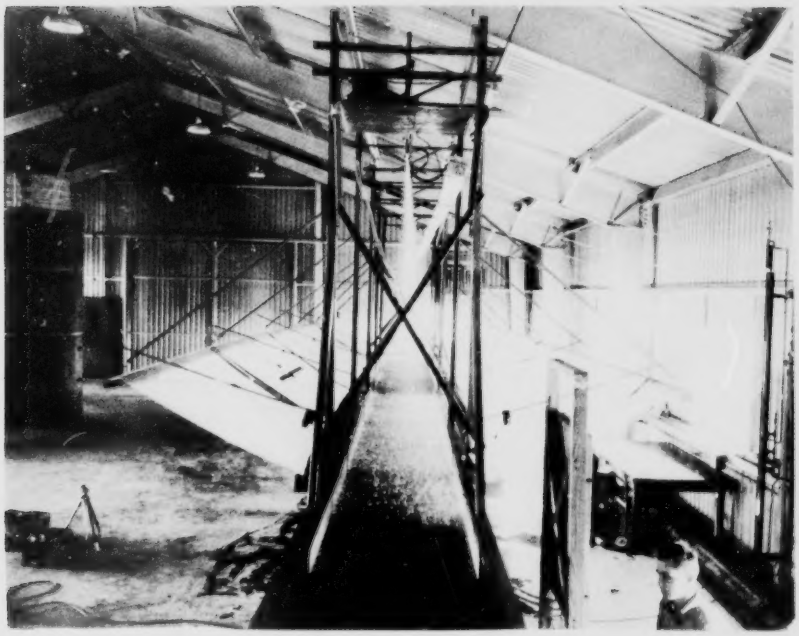

FIGURE 9. FLOW IN RESEARCH FLUME WITH SIMULATED RAINFALL

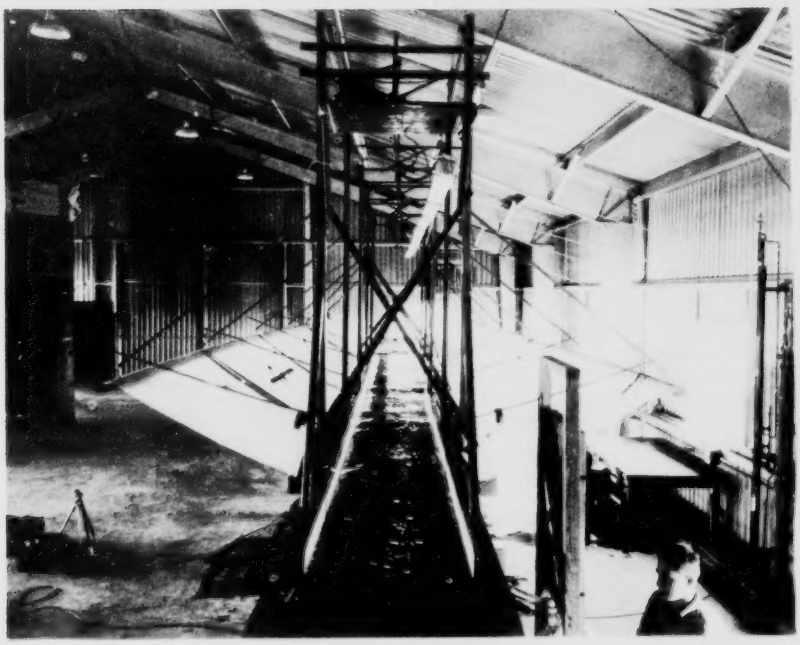

FIGURE 10. FLOW IN RESEARCH FLUME WITHOUT SIMULATED RAINFALL

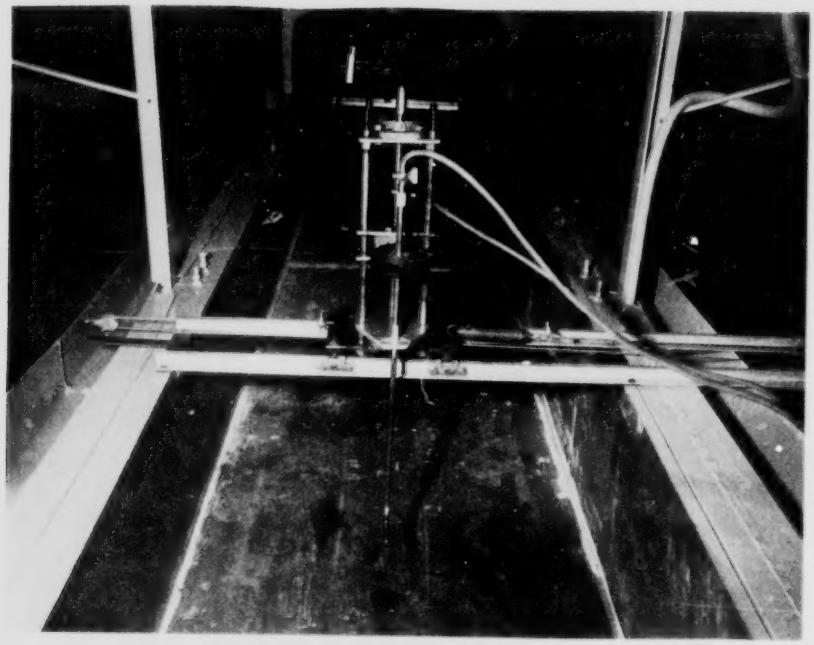

FIGURE 11. TRAVERSING MECHANISM AND PRANDTL TUBE POSITIONED IN THE RESEARCH FLUME

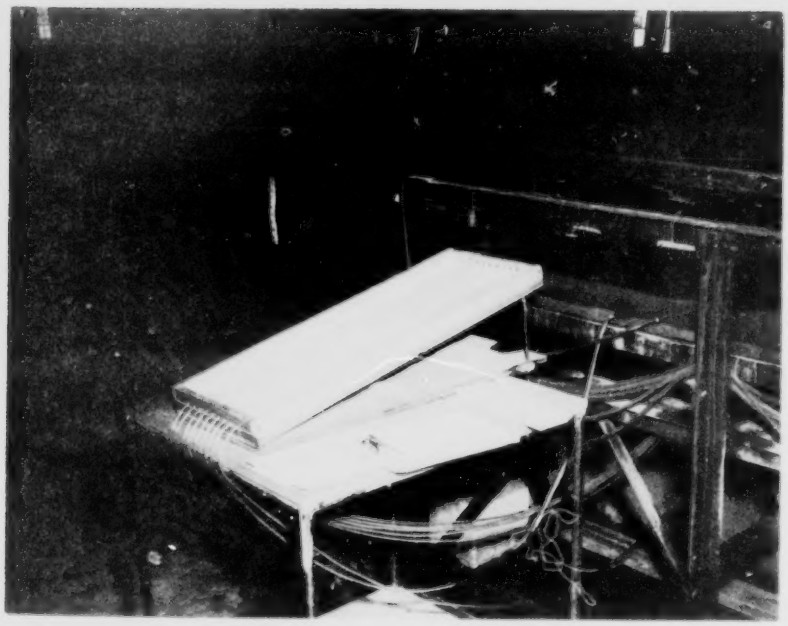

FIGURE 12 INCLINED WATER-TO-AIR MANOMETER USED TO MEASURE THE POINT VELOCITIES WITHIN THE FLOW

vertical as well as laterally across the flume. This permitted point velocity readings to be taken at any point in the cross-section of the flow. The static and dynamic velocity connections of the Prandtl tube were connected (with transparent Tygon tubing) to an inclined manometer having a scale magnification of 5 shown in Figure 12. Tests were also run using a total head velocity probe and a Pitot-static tube. All three probes are illustrated in Figure 13.

Procedure

Preliminary tests for obtaining point velocity readings in the entire cross section of the flume were made. The tests were run with flow depths of 0.1, 0.2, 0.3, and 0.5 feet. All tests were conducted with the flume grade equal to 0.001. The water was admitted into the flume until the desired depth was obtained. As the flow was approaching an equilibrium condition, the inclined manometer and the series of manometers for the velocity profile were primed. Priming the air-to-water manometers was accomplished by forcing water under pressure through the manometers and tubing to the flume removing any entrapped air that might have been in the lines.

After equilibrium was established, point velocity readings were taken at the 0.125, 0.25, 0.33, 0.50, 0.67, 0.75, and 0.875 points across the flume. Depth readings were taken at 0.1, 0.2, 0.4, 0.6, 0.8 and 0.9 of the depth of flow measured from the surface of the water. This data was then plotted to determine if horizontal shear occurred across the center of the flume. Rainfall was also applied at each of the depths

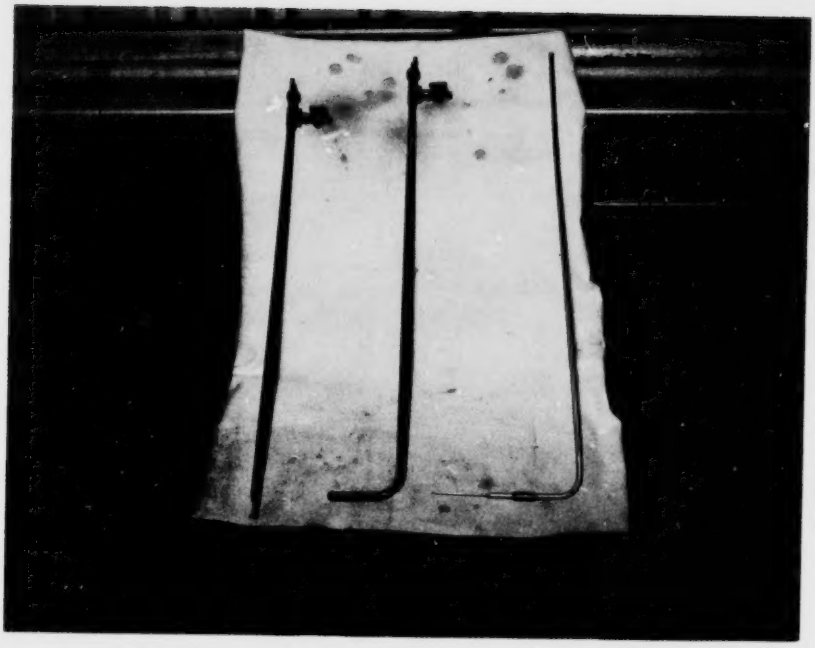

FIGURE 13 THE THREE VELOCITY SENSING PROBES: PITOT-STATIC TUBE, PRANDTL TUBE, AND THE TOTAL HEAD TUBE

to determine if the rainfall striking the water surface would create cross currents and thus cause horizontal shear to take place across the centerline of the flume.

After this analysis was made, the Prandtl tube was located at the center of the flume or very near the center where no horizontal shear occurred. At this traverse position, velocity measurements were taken at depths of 0.046d, 0.097d, 0.155d, 0.30d, 0.522d, 0.7d, and 0.9d below the water surface where d is the total depth of flow. For depths of flow of 0.1 feet and 0.2 feet neither the 0.046d nor the 0.9d reading could be obtained, due to air entering the Prandtl tube at 0.046d and the tube striking the bottom before reaching 0.9d. The readings were taken at 0.1-foot increments for depths of flow between 0.1 and 0.5 feet. Readings were taken at each depth with and without rainfall. The flow rates were kept constant for each flow depth. This required some adjustments of the flow entering the flume especially for the shallower depths, since the water from the rainfall simulator contributed to the total flow and consequently the depth of flow.

A second series of tests was run using a total head probe constructed from 0.065-inch outside diameter stainless steel hypodermic tubing. Point velocities were taken at 0.1, 0.2, 0.3, 0.5, 0.7, 0.8 and 0.9 of the depth of flow at the center of the flume. The static reading was obtained from a wall piezometer located at the same longitudinal position along the flume at the tip of the velocity probe. The velocity coefficient of the total head probe was obtained by two methods.

One method was determining the velocity by observing the time required for a small disk of cork to travel 50 feet. An average time was used for 5 runs. The surface velocity was measured with the total head probe for each run by locating the probe as near the surface as possible without entraining air in the lines connecting the probe to the manometer. The velocity coefficient was also obtained by determining the total rate of flow by integrating the point velocity readings across the width of flow and comparing with the total discharge measured by the H-type flow rate measuring flume. The average of the two velocity coefficients was used.

The third and fourth series of tests were made using a smooth marine plywood bed using the Prandtl tube and a Pitot-static tube, respectively. This was done by removing the concrete slabs in the flume. For these series, depths of flow used were 0.2, 0.3, and 0.4 feet. Point velocities were taken by the same procedure as the previous series of tests. The velocity coefficient for the Pitot-static tube was also determined in the manner stated previously.

# CHAPTER IV

## DATA ANALYSES AND DISCUSSION OF RESULTS

The primary objective of this study was to determine the effect of rainfall on the vertical velocity distribution of shallow channel flow. The first step in the study was to determine how closely the velocity distribution without simulated rainfall compared with previous studies and the theoretical equations developed. The velocity distribution across the flume was first determined from point velocity readings across the flume. Point velocity readings were also taken with simulated rainfall applied to the water surface. Isovels were drawn for the flow and showed that the flow in the center of the flume may be analyzed as being in an infinitely wide channel. A typical velocity distribution for 0.3 feet depth of flow with and without simulated rainfall is shown in Figures 14 and 15, respectively. The simulated rainfall intensity distribution pattern across the flume is also shown in Figure 14 above the cross-section of flow.

### Velocity distribution without rainfall

Four series of tests were conducted without simulated rainfall. Two pairs of tests were made each on a concrete bed and on a plywood bed. The data were analyzed using an IBM 709 computer. Regression analyses were made to determine the constants A and E of

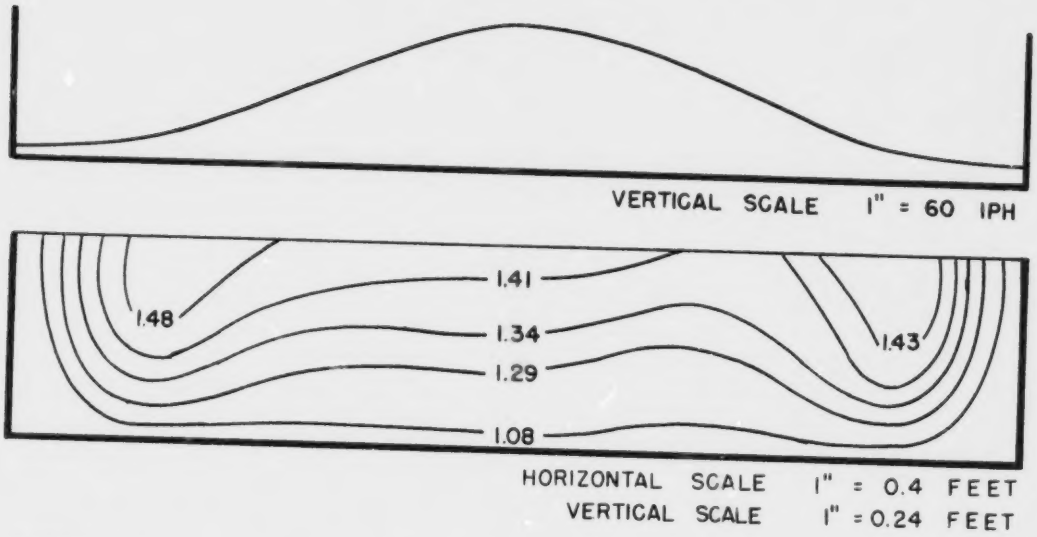


FIGURE 14 RAINFALL PATTERN AND RESULTING CROSS-SECTIONAL VELOCITY DISTRIBUTION FOR 0.3 FEET DEPTH OF FLOW

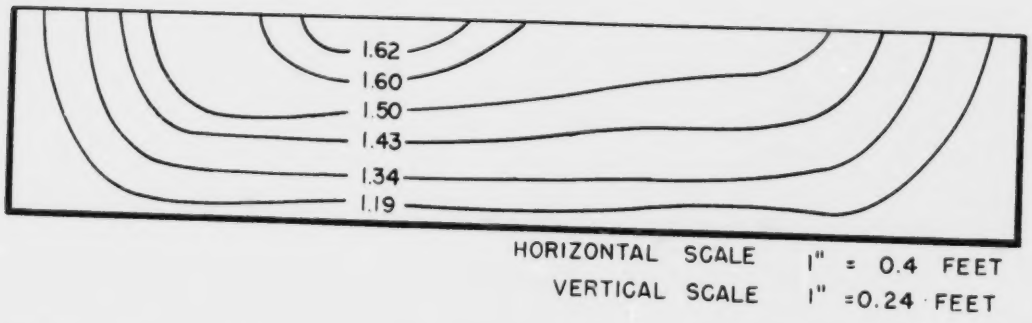


FIGURE 15. CROSS-SECTIONAL VELOCITY DISTRIBUTION FOR 0.3 FEET DEPTH OF FLOW WITHOUT SIMULATED RAINFALL

the general expression

$$\frac{v - V}{\sqrt{gdS}} = A \log_{10} \frac{y}{d} + E \qquad (22)$$

which is of identical form to the theoretical equation 14.

All terms in equation 22 were measured except A, E, and V. Before the regression analyses were made to determine A and E in equation 22, the mean velocity, V, was determined. The mean velocity for each flow depth was determined by integrating a regression line determined from the point velocities, when the point velocities were plotted versus the logarithm of the depth above the bed. The mean velocity was obtained by dividing the integrated expression by the total depth of flow. The regression lines obtained for no rainfall are plotted in Figure 16-20.

From equation 14, the theoretical equation, the constants A and E are 5.75 and 2.5, respectively. A goodness of fit test was also made for each series of tests. The constants and goodness of fit are given in Table 1. Also included in the analyses are velocity distribution data obtained from research conducted by Smerdon as part of a critical tractive force study on the soil bed of channels (12). The results from the Smerdon data, which were obtained using a Darcy tube velocity sensing probe, are also included in Table 1.

The difference in regression equations was small with the exception of the Prandtl tube data on the plywood bed. No explanation can be given for the difference. Differences were also present between the constants of the theoretical equations and the regression equations. Although the

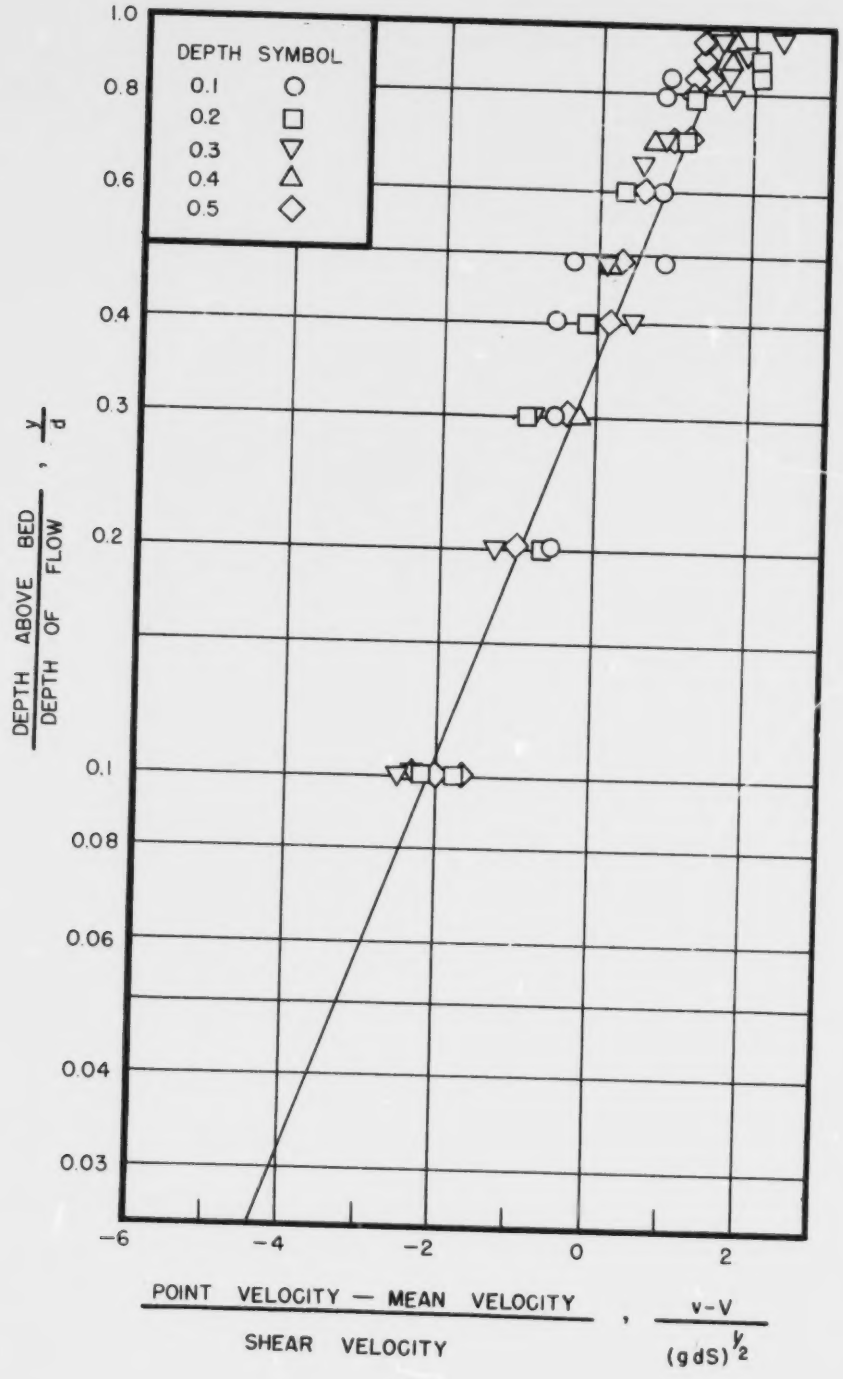


FIGURE 16. VELOCITY DISTRIBUTION REGRESSION CURVE USING THE PRANDTL TUBE WITHOUT SIMULATED RAINFALL ON A CONCRETE BED

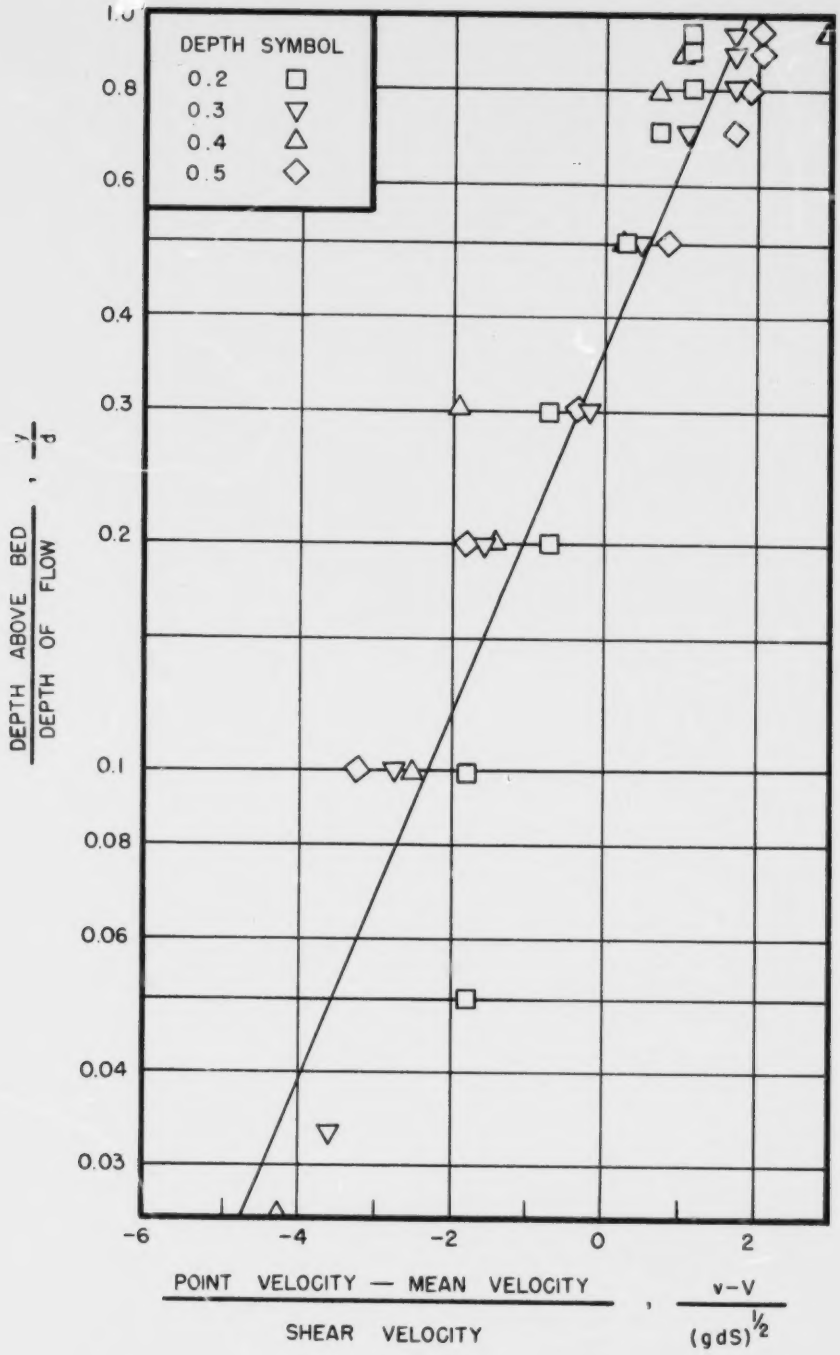


FIGURE 17. VELOCITY DISTRIBUTION REGRESSION CURVE USING THE TOTAL HEAD TUBE WITHOUT SIMULATED RAINFALL ON A CONCRETE BED

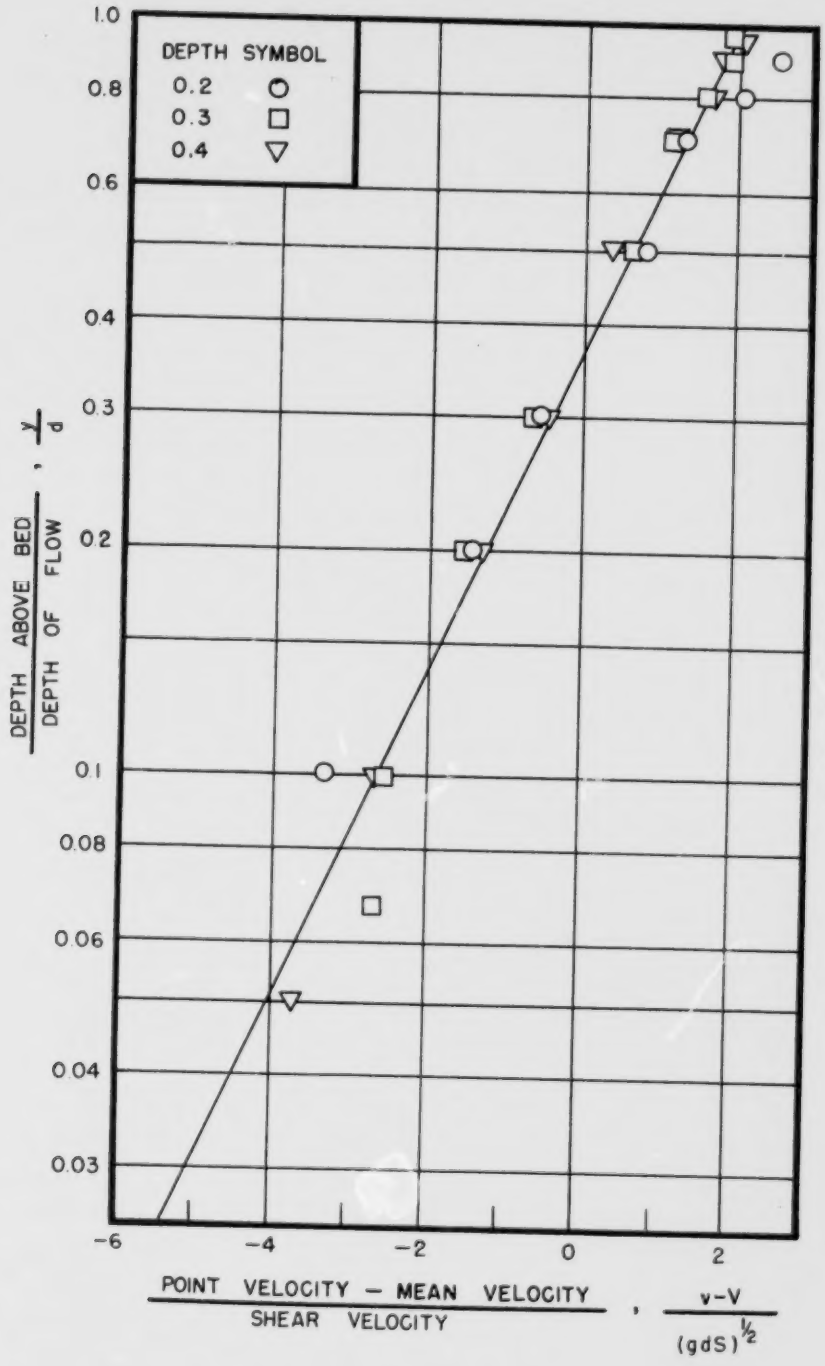


FIGURE 18. VELOCITY DISTRIBUTION REGRESSION CURVE USING THE PRANDTL TUBE WITHOUT SIMULATED RAINFALL ON A PLYWOOD BED

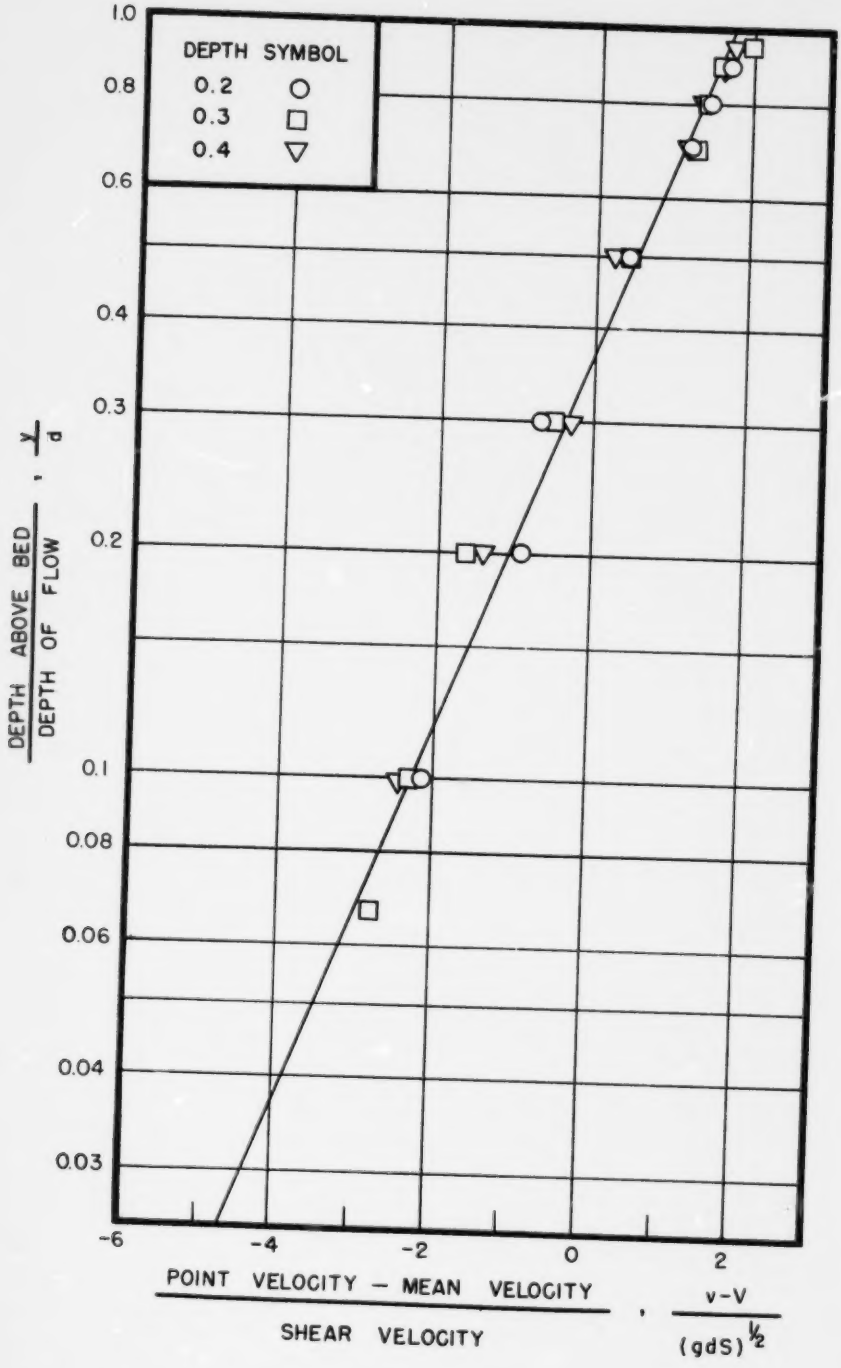


FIGURE 19. VELOCITY DISTRIBUTION REGRESSION CURVE USING THE PITOT-STATIC TUBE WITHOUT SIMULATED RAINFALL ON A PLYWOOD BED

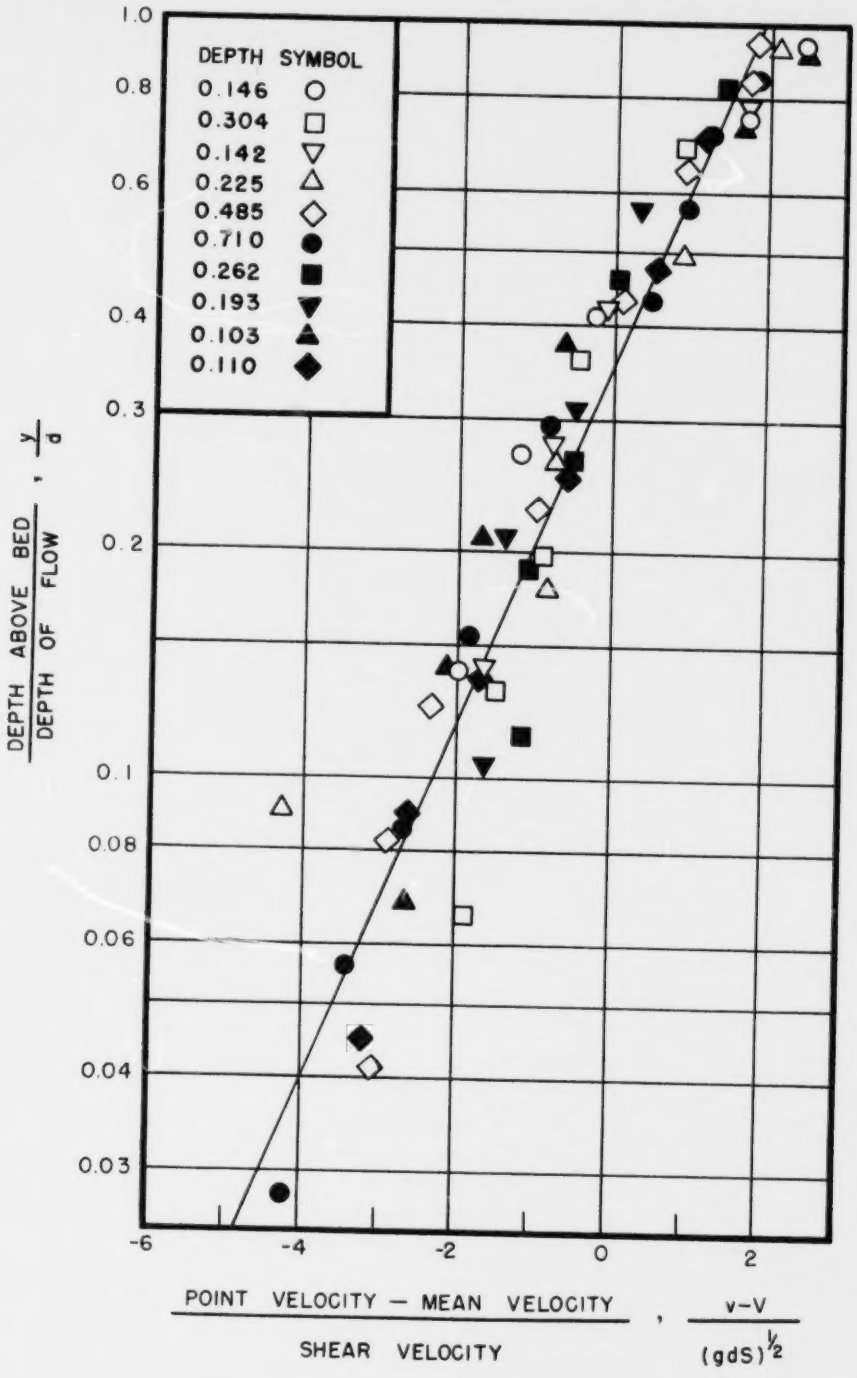


FIGURE 20. VELOCITY DISTRIBUTION REGRESSION CURVE FROM SMERDON DATA USING A DARCY TUBE WITHOUT SIMULATED RAINFALL ON A SOIL BED.

TABLE I. REGRESSION ANALYSIS RESULTS OF EQUATION 22 FOR TESTS CONDUCTED WITHOUT SIMULATED RAINFALL.

| Sensing Probe | A | E | N | F | Significance Level |
|---|---|---|---|---|---|
| | | CONCRETE BED | | | |
| Prandtl | 3.824 | 1.646 | 83 | 1123.6 | 0.001 |
| Total head | 4.174 | 1.806 | 37 | 275.9 | 0.001 |
| | | PLYWOOD BED | | | |
| Prandtl | 4.720 | 2.064 | 25 | 841.3 | 0.001 |
| Pitot-static | 4.013 | 1.746 | 25 | 1176.6 | 0.001 |
| | | SOIL BED | | | |
| Darcy | 4.170 | 1.850 | 62 | 817.3 | 0.001 |

A = slope of regression line

E = intercept of regression line at $\log_{10} \frac{y}{d} = 0$

N = number of readings included in the regression

F = statistic test for goodness of fit

regression constants and theoretical constants differed, all regression analyses were significant at greater than the 0.001 level.

Velocity distribution with rainfall

Similar tests were run with simulated rainfall to determine the effect of rainfall on the velocity distribution in shallow channel flow. An assumption was made that the velocity distribution with simulated rainfall would follow a logarithmic distribution.

Regression analyses were made to determine the constants of equation 22 for each of the tests. The results are given in Table II. The regression equations were all significant at greater than the 0.001 level, although a larger variation occurred between the regression constants with simulated rainfall than without simulated rainfall. The regression equations are shown in Figures 21-24.

The intercept values and the slopes of the regression lines each decreased, indicating the following: (1) a decrease in the surface velocity, (2) a decrease in the velocity gradient.

Shear at the bed. The shear at the bed of the channel was reduced by simulated rainfall in all of the tests. A paired comparison of the regression line plots without rainfall (Figures 16-19) and with rainfall (Figures 21-24) indicates the magnitude of the reduction of the shear at the bed.

The reduced shear at the bed resulting from the decrease in the velocity gradient has been discussed by Smerdon (11). Results from his

TABLE II. REGRESSION ANALYSIS RESULTS OF EQUATION 22 FOR TESTS CONDUCTED WITH SIMULATED RAINFALL.

| Velocity Sensing Probe | A | E | N | F | Significance Level |
|---|---|---|---|---|---|
| | | CONCRETE BED | | | |
| Prandtl | 2.860 | 1.257 | 78 | 371.1 | 0.001 |
| Total head | 3.616 | 1.572 | 33 | 483.2 | 0.001 |
| | | PLYWOOD BED | | | |
| Prandtl | 4.647 | 2.038 | 24 | 544.2 | 0.001 |
| Pitot-static | 3.883 | 1.685 | 24 | 1088.0 | 0.001 |

A = slope of the regression line

E = intercept of regression line at $\log_{10} \frac{y}{d} = 0$

N = number of readings included in the regression

F = statistic test for goodness of fit

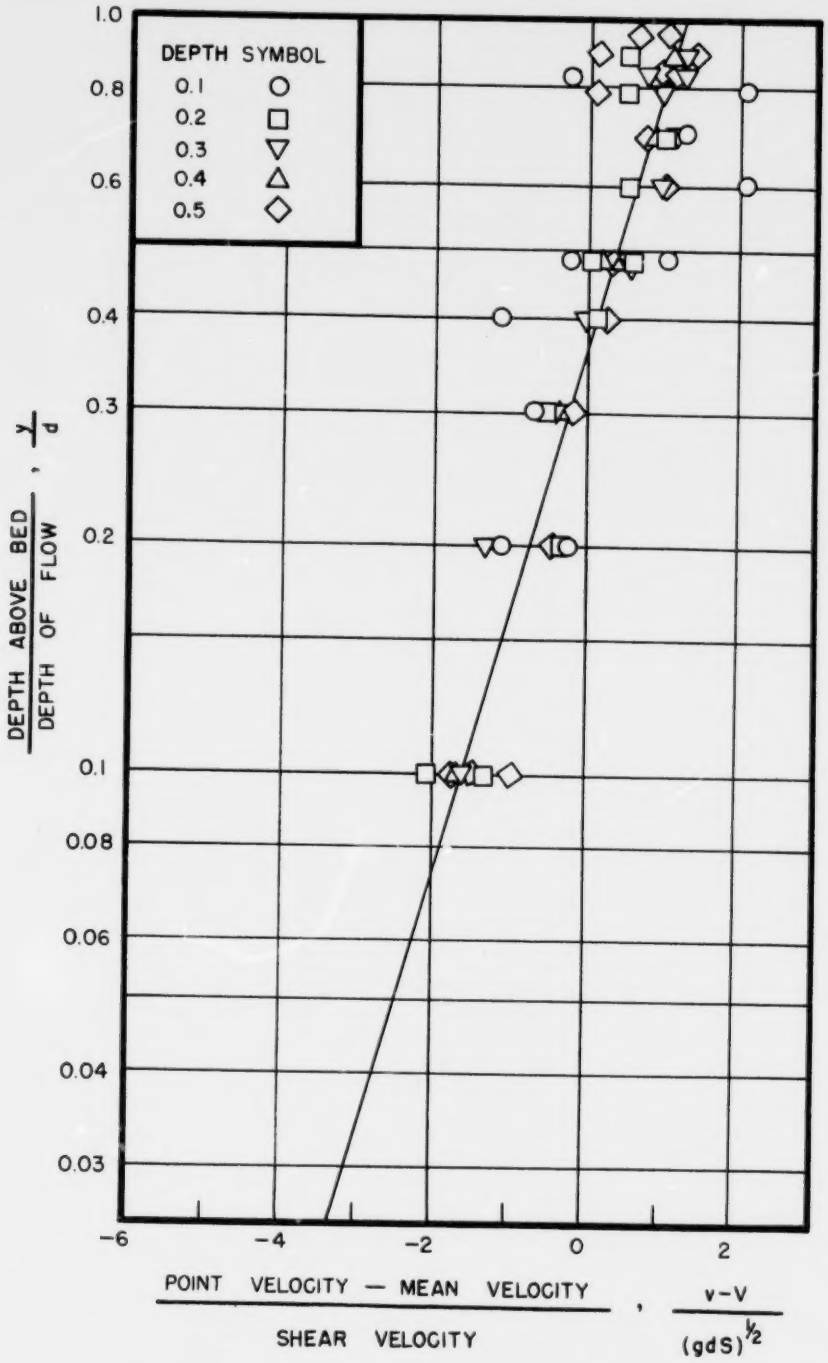


FIGURE 21 . VELOCITY DISTRIBUTION REGRESSION CURVE USING THE PRANDTL TUBE WITH SIMULATED RAINFALL ON A CONCRETE BED

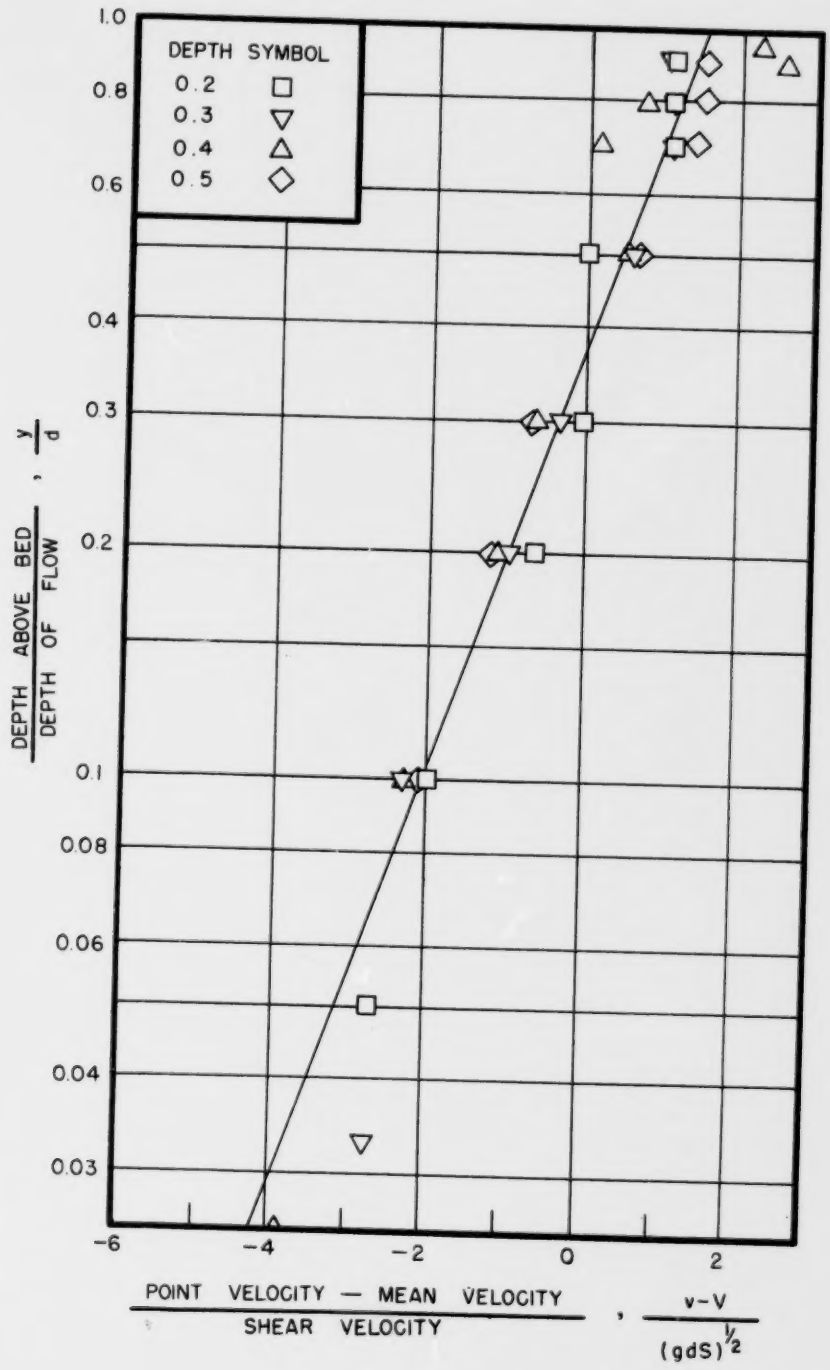


FIGURE 22 . VELOCITY DISTRIBUTION REGRESSION CURVE USING THE TOTAL HEAD TUBE WITH SIMULATED RAINFALL ON A CONCRETE BED

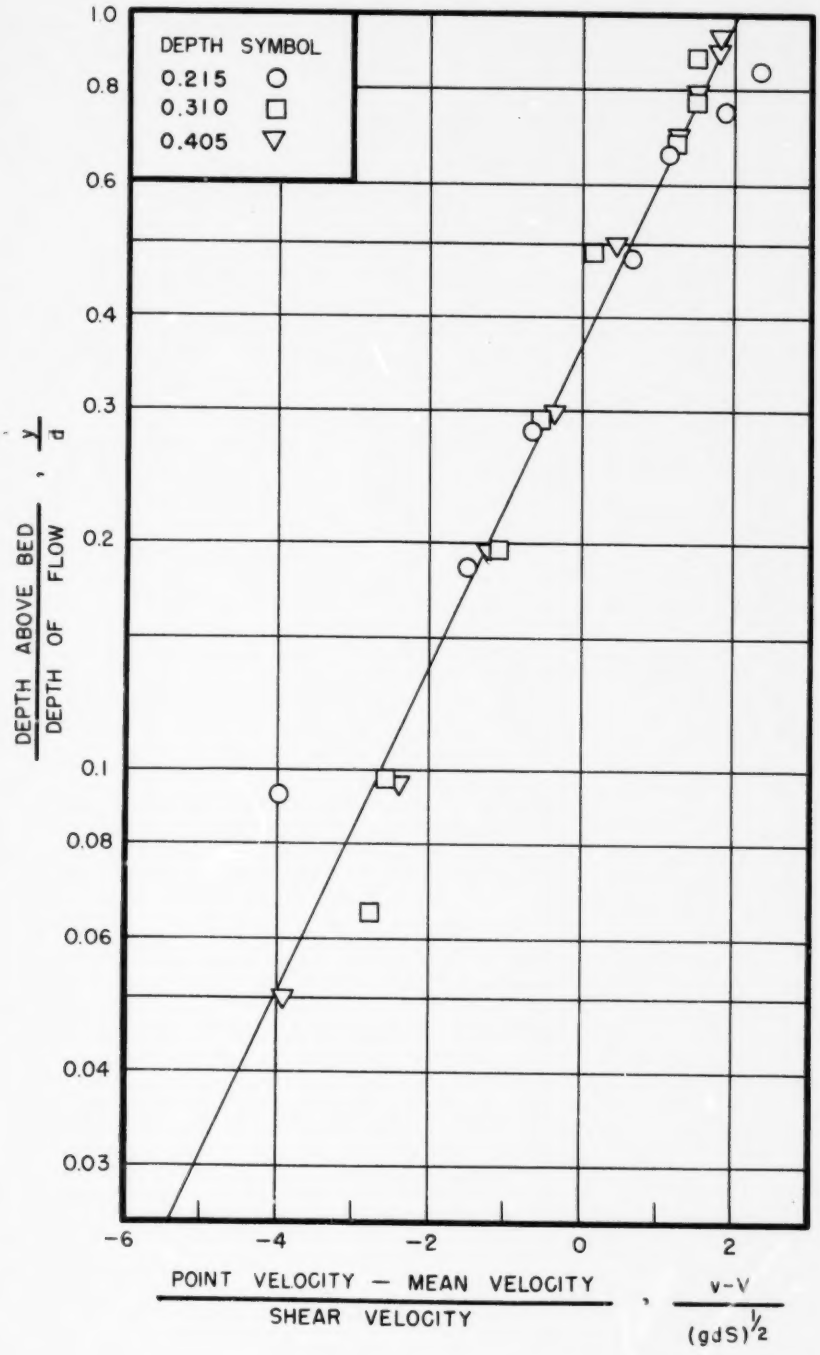


FIGURE 23. VELOCITY DISTRIBUTION REGRESSION CURVE USING THE PRANDTL TUBE WITH SIMULATED RAINFALL ON A PLYWOOD BED

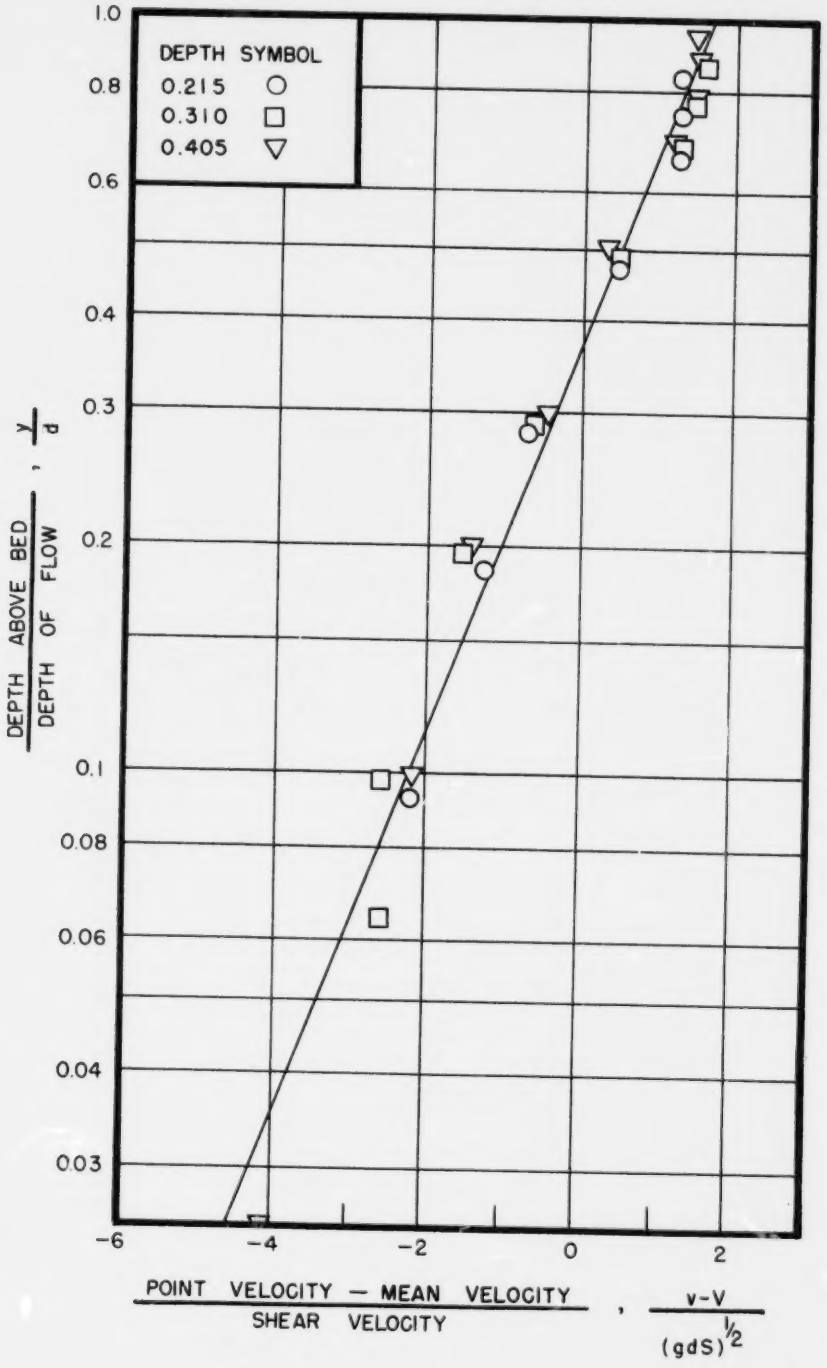


FIGURE 24 . VELOCITY DISTRIBUTION REGRESSION CURVE USING THE PITOT-STATIC TUBE WITH SIMULATED RAINFALL ON A PLYWOOD BED

study showed that simulated rainfall generally reduced the amount of sediment carried in the flow. The results from this study indicate a reduction in the velocity gradient by simulated rainfall, thus supporting Smerdon's results concerning suspended sediment transport.

Resistance coefficient. The resistance coefficient was calculated for each series of tests in equation 19. These values are listed in Tables VI - XIV in the Appendix.

Regression analyses were also made of the general expression

$$\frac{\frac{v}{V} - 1}{\sqrt{f}} = G \log_{10} \frac{y}{d} + H \qquad (23)$$

in which G and H are constants. Equation 23 is analogous to equation 21, the theoretical equation. The values of G and H including the statistical significance of the regressions are given in Tables III and IV. The values of the constants obtained deviate from the theoretical values in equation 21 in the same manner as the values of the constants obtained for equation 22 deviated from the theoretical values in equation 14. This was to be expected because the analyses are essentially the same.

It is interesting to note that Vanoni (14) concluded the resistance decreased due to suspended sediment in the flow, but results from this study showed that the friction resistance increased slightly with simulated rainfall on the concrete bed. There was no significant difference, however, for the plywood bed as may be found in Tables VI - XIV of the Appendix.

TABLE III. REGRESSION ANALYSIS RESULTS OF EQUATION 23 FOR TESTS CONDUCTED WITHOUT SIMULATED RAINFALL.

| Velocity Sensing Probe | G | H | N | F | Significance Level |
|---|---|---|---|---|---|
| | | CONCRETE BED | | | |
| Prandtl | 1.352 | 0.582 | 83 | 1123.6 | 0.001 |
| Total head | 1.476 | 0.639 | 37 | 275.9 | 0.001 |
| | | PLYWOOD BED | | | |
| Prandtl | 1.669 | 0.730 | 25 | 841.3 | 0.001 |
| Pitot-static | 1.419 | 0.617 | 25 | 1176.6 | 0.001 |
| | | SOIL BED | | | |
| Darcy | 1.474 | 0.654 | 62 | 820.9 | 0.001 |

G = slope of the regression line

H = intercept of the regression line at $\log_{10} \frac{y}{d} = 0$

N = number of readings included in the regression

F = statistic test for goodness of fit

TABLE IV. REGRESSION ANALYSIS RESULTS OF EQUATION 23 FOR TESTS CONDUCTED WITH SIMULATED RAINFALL.

| Velocity Sensing Probe | G | H | N | F | Significance Level |
|---|---|---|---|---|---|
| | | CONCRETE BED | | | |
| Prandtl | 1.011 | 0.444 | 78 | 371.1 | 0.001 |
| Total head | 1.279 | 0.556 | 33 | 483.2 | 0.001 |
| | | PLYWOOD BED | | | |
| Prandtl | 1.643 | 0.720 | 24 | 544.2 | 0.001 |
| Pitot-static | 1.373 | 0.596 | 24 | 1088.0 | 0.001 |

G = slope of the regression line

H = intercept of the regression line at $\log_{10} \frac{y}{d} = 0$

N = number of readings included in the regression

F = statistic test for goodness of fit

Discussion of variation in results from the theoretical

Vanoni (14) indicates that the von Karman universal constant depends only on the mechanism of turbulent mixing. Therefore, any change in the turbulent mixing would affect the value of $K$. The turbulent mixing is characterized by the kinematic eddy viscosity, $\epsilon$ which is also known as the turbulent momentum transfer coefficient denoted as $\epsilon_m$. A direct relationship exists between $\epsilon$ and $K$ which may be shown by substituting $\epsilon \rho = \eta$ in equation 1b and combining with equation 2 yielding

$$\epsilon = Ky \frac{\tau}{\rho \sqrt{\tau_o / \rho}}$$

Vanoni (14) further states that for a reduction of $\epsilon$, then $K$ must also decrease if the shear and depth remain constant. From equation 1b, the velocity gradient must increase for a decrease in $\epsilon$, thus increasing the velocity of the flow.

Evaluating $K$ from the slope A of Table I, values range from 0.487 to 0.602 without simulated rainfall. From Table II, $K$ varies from 0.495 to 0.805 with simulated rainfall. The accepted value for $K$ of 0.40 was greatly exceeded, indicating a large difference in the turbulent mixing mechanism. It should be noted that the average of the experimental values of the universal constant, $K$, from these tests, without rainfall, was 0.553 compared to 0.552 obtained from tests conducted by Smerdon (12). An explanation for the large $K$ values compared to similar previous research (5, 14) in open channels cannot be given. A complete understanding of the turbulent mixing in the flow is needed to give an explanation of the higher values.

The average $K$ for the tests with simulated rainfall was 0.633. The increased value of $K$ means an increase in the kinematic eddy viscosity or turbulent momentum transfer coefficient. A decrease in velocity must also occur if the shear remains constant. The shear at the bed, however, was decreased, but in Tables VI - XIV, the mean velocities with simulated rainfall were also generally reduced from the velocities without simulated rainfall. Therefore, a combination of shear reduction and a decrease in mean velocity may be expected when simulated rainfall is added to shallow channel flow.

Discussion of variation between tests

The variation in results with simulated rainfall and without simulated rainfall are assumed to be relative. The variations may be attributed to (a) nonuniform flow conditions in some of the tests, (b) the assumption of an infinitely wide channel not completely satisfied, and (c) instrumentation error.

Nonuniform flow. Uniform flow occurred only for the tests with 0.5 feet depth when the Prandtl tube was used, and the 0.1 feet and 0.5 feet depth when the total head tube was used. These were with the concrete bed without simulated rainfall. With simulated rainfall, uniform flow occurred at 0.3 and 0.4 feet depth for both the Prandtl tube and total head probe on the concrete bed. Uniform flow was maintained for all depths on the plywood bed with and without simulated rainfall. All of the Smerdon data were also obtained with uniform flow conditions. Comparison of the regression constants showed less variation between uni-

form and nonuniform flow conditions than within tests for either flow condition, excluding the Prandtl data on the plywood bed.

Infinitely wide channel. Preliminary tests were conducted to determine the flow conditions at the center of the flume. Horizontal isovels at the center of the flume indicated that the channel flow could be analyzed as an infinitely wide channel as shown in Figure 15. These tests were made with the Prandtl tube only on the concrete bed, however. Bazin (5) stated that flow in rectangular channels may be analyzed as being infinitely wide when the bottom width is greater than five times the depth of flow. Therefore, all other tests were assumed to have the same pattern of isovels.

Instrumentation error. Three velocity sensing probes were used to measure the point velocities within the flow. All velocity readings were made with a water-to-air inclined manometer having a multiplication factor of 5.0. The manometer could be read to 0.01 feet and estimated to the nearest 0.005 feet. A variation of 0.005 feet in the manometer reading caused a variation in the calculated velocity of 0.0802 feet per second or a variation of approximately four per cent for any point velocity recorded in this study. The possible magnitude of variation in the point velocities could not encompass the difference between the theoretical constants and the regression constants for equation 22. Assuming a normal distribution about the true point velocity, other sources of error would be present. The high significance level of the regresssions (Tables I and II) supports the assumption of a normal distribution about

the true point velocities.

The static reading used for the total head probe was obtained from a piezometer opening in the channel wall at the location of the velocity sensing probe. Data obtained from the Prandtl tube indicated a static reading approximately 0.006 feet less than the reading obtained from the wall piezometer. The difference in readings is another source of variation in the results.

Static readings obtained from the Pitot-static tube varied slightly throughout each test conducted at a constant depth. For any given depth of flow, the static reading should be constant, assuming a fixed reference plane. Therefore, the static readings from the Prandtl tube data were used since both sensing probes were used under similar flow conditions.

The variation of the static readings from the Pitot-static tube may be partially explained by analyzing the sensing probe as a flat plate at zero incidence to the flow. Schlicting (11) states that the boundary layer in the vicinity of the leading edge of a flat plate at zero incidence is always laminar flow. The critical Reynolds number, the value at which the boundary layer becomes turbulent, is between 500,000 and 3,000,000 for flat plates at zero incidence (11). The Reynolds number for the flow past the sensing probe varied from 3100 to 6000 using the distance from the sensing probe tip to the static openings as the characteristic length. The small variations in the static readings may be attributed to the variation in the viscous forces occurring at the static openings.

Statistical analysis of the data

Analysis of variance tests were made on the regression lines to determine if there was a significant difference between tests conducted with and without simulated rainfall. Analyses were also made to determine the effect of different velocity sensing probes and bed conditions on the tests.

A summary of the analyses is given in Table V. Only five of the ten comparisons proved to be significantly different at the 0.01 level. Of the three comparisons for the effect of rainfall, only the Prandtl velocity sensing probe used on a concrete bed condition was significant at the 0.01 level. This indicates there was little effect on the velocity distribution due to simulated rainfall. There was a significant difference between bed conditions with and without simulated rainfall using the Prandtl velocity sensing probe indicating that the bed condition has a definite effect on the velocity distribution. A significant difference was also indicated between the Prandtl velocity sensing probe and the Darcy sensing probe used by Smerdon. An added effect due to the Prandtl probe used on a concrete bed condition and the Darcy probe used on a soil bed condition may be responsible for the significant difference in these velocity sensing probes.

TABLE V. SUMMARY OF ANALYSIS OF VARIANCE TESTS BETWEEN VARIABLE COMPARED.

| Tests Compared Data Group Nos. | Variable Compared | Significance Level of Difference | Analysis in Table |
|---|---|---|---|
| 1 with 2 | Rainfall | 0.01 | XV |
| 3 with 4 | Rainfall | NS | XVI |
| 5 with 6 | Rainfall | NS | XVII |
| 7 with 8 | Rainfall | NS | XVIII |
| 1 with 5 | Bed Condition | 0.01 | XIX |
| 2 with 6 | Bed Condition | 0.01 | XX |
| 1 with 3 | Velocity Probe | NS | XXI |
| 5 with 7 | Velocity Probe | 0.01 | XXII |
| 1 with 9 | Velocity Probe | 0.01 | XXIII |
| 5 with 9 | Velocity Probe & Bed Condition | NS | XXIV |

Concrete Bed

(1) Prandtl velocity probe--without rainfall
(2) Prandtl velocity probe--with rainfall
(3) Total head velocity probe--without rainfall
(4) Total head velocity probe--with rainfall

Plywood Bed

(5) Prandtl velocity probe--without rainfall
(6) Prandtl velocity probe--with rainfall
(7) Pitot-static velocity probe--without rainfall
(8) Pitot-static velocity probe--with rainfall

Soil Bed

(9) Darcy velocity probe--without rainfall

# CHAPTER V

## SUMMARY AND CONCLUSIONS

Vertical velocity distribution affects the suspended sediment transport capacity of streams. In shallow streams, where rainfall has a definite effect on the velocity distribution of the flow, the suspended sediment transport capacity is likely changed.

Studies were conducted in a research flume with and without simulated rainfall on shallow flow to evaluate the effect of rainfall on velocity distributions. Tests were conducted with five depths of flow on a roughened concrete flume bed (to simulate the roughness of a natural channel) and three depths of flow with a smooth plywood bed. Three different velocity sensing probes were used: a Prandtl tube, a total head tube, and a Pitot-static tube.

Regression analyses were performed on the vertical velocity distribution data and compared to theoretical equations. All regressions were highly significant, although a large difference occurred between the theoretical equations and the regression equations.

Tests with simulated rainfall indicated a decrease in surface velocity and a decrease in the velocity gradient.

The following conclusions were made from this study:

1. Simulated rainfall retards the velocity near the surface and reduces the velocity gradient of the flow.

2. The relative depth at which the point velocity was equal to the mean velocity was not suppressed due to the simulated rainfall striking the water surface.
3. The velocity distribution of flow with simulated rainfall may be analyzed using a logarithmic velocity distribution as shown by the high level of significance for the regression of the velocity distribution.

During the course of this study the need for the following future studies became apparent:

1. Flume slope should be varied to determine if slope has an effect on the constants in the general velocity distribution equation.
2. A highly sensitive velocity probe and indicating manometer are needed to reduce the possible instrumentation errors.
3. Rainfall intensity should be varied to develop a relationship between the reduction of the surface velocity, velocity gradient, and the intensity of the simulated rainfall.

# BIBLIOGRAPHY

1. Bennett, H. H. Soil conservation. McGraw-Hill Book Company, Inc., New York, 1939.

2. Brown, C. B. The control of reservoir silting. USDA MP521 Washington: Government Printing Office, 1943.

3. Brown, C. B. Sediment transportation. Chapter XII of Engineering Hydraulics, John Wiley and Sons, Inc., New York, 1950.

4. Chow, V. T. Open channel hydraulics. McGraw-Hill Book Company, Inc., New York, 1959.

5. Keulegan, H. G. Laws of turbulent flow in open channels. U. S. Bureau of Standards Journal of Research, 21:707-741, RP1151, December, 1938.

6. Leliavsky, S. Historic development of the theory of flow in canals and rivers. The Engineer, 191:466-468, 1951.

7. Meyer, L. D. An investigation of methods for simulating rainfall on standard runoff plots and a study of the drop size, velocity, and kinetic energy of selected spray nozzles. Special Report No. 81, USDA-ARS, May, 1958.

8. Mutchler, C. K. and L. F. Hermsmier. Review of rainfall simulators. Paper No. 63-726 presented at the 1963 Winter Meeting, ASAE, Chicago, Illinois, December 10-13, 1963.

9. Rouse, H. Elementary mechanics of fluids. John Wiley and Sons, Inc., New York, 1946.

10. Schlicting, H. Boundary layer theory. Translated by J. Kestin, McGraw-Hill Book Company, Inc., New York, 4th Edition, 1960.

11. Smerdon, E. T. Effect of rainfall on critical tractive forces in channels with shallow flow. Paper No. 63-700 presented at the 1963 Winter Meeting, ASAE, Chicago, Illinois, December 10-13, 1963.

12. Smerdon, E. T. The tractive force theory applied to the stability of open channels in cohesive soils. Ph.D. dissertation, University of Missouri, 1959.

13. Vanoni, V. A. Velocity distribution in open channels. Civil Engineering, 11:356-357, June, 1941.

14. Vanoni, V. A. Transportation of suspended sediment by water. Trans. ASCE, 111:67-133, 1946.

15. Wang, C. T. On the velocity distribution of turbulent flow in pipes and channels of constant cross section. Journal of Applied Mechanics, 13:A85-A90, 1946.

# APPENDIX

# LIST OF SYMBOLS

| Symbol | | Dimension |
|---|---|---|
| A | slope of regression line | |
| b | width of the channel | L |
| B | constant | |
| $C_1$ | constant | |
| $C_2$ | constant | |
| $C_3$ | constant | |
| $C_f$ | mean drag coefficient | |
| d | total depth of flow | L |
| D | depth of flow without simulated rainfall | L |
| E | intercept of regression line at $\log_{10} \frac{y}{d} = 0$ | |
| f | Darcy-Weisbach resistance coefficient | |
| F | statistics test for goodness of fit | |
| g | acceleration of gravity | $LT^{-2}$ |
| G | slope of regression line | |
| H | intercept of regression line at $\log_{10} \frac{y}{d} = 0$ | |
| k | roughness of the boundary | L |
| l | eddy size | L |
| N | number of readings included in the regression | |
| q | discharge per unit width of flow | $L^2T^{-1}$ |

| Symbol | | Dimension |
|---|---|---|
| $Q$ | total discharge of flow | $L^3T^{-1}$ |
| $S$ | energy gradient | |
| $v$ | velocity at any depth above the channel bed | $LT^{-1}$ |
| $v_o$ | velocity at the nominal limit of the boundary layer | $LT^{-1}$ |
| $\bar{v}$ | temporal mean value of the velocity | $LT^{-1}$ |
| $v_{max}$ | maximum velocity in the vertical | $LT^{-1}$ |
| $V$ | mean velocity without rainfall | $LT^{-1}$ |
| $V_R$ | mean velocity with rainfall | $LT^{-1}$ |
| $y$ | distance above the channel bed | $L$ |
| $y'$ | value of y at which the logarithmic velocity distribution curve intersects the axis | $L$ |
| $\gamma$ | specific weight | $FL^{-3}$ |
| $\delta$ | distance from boundary to the zone differentiating between laminar and turbulent flow | $L$ |
| $\epsilon$ | kinematic eddy viscosity | $L^2T^{-1}$ |
| $\epsilon_m$ | turbulent momentum transfer coefficient | $L^2T^{-1}$ |
| $\eta$ | eddy viscosity | $FL^{-2}T$ |
| $\kappa$ | von Karman's universal constant | |
| $\mu$ | dynamic viscosity | $FL^{-2}T$ |
| $\nu$ | kinematic viscosity | $L^2T^{-1}$ |
| $\rho$ | mass density of the flowing media | $FL^{-4}T^2$ |
| $\tau$ | intensity of shear | $FL^{-2}$ |
| $\tau_o$ | intensity of shear at a boundary | $FL^{-2}$ |
| $\chi$ | stability parameter | |

TABLE VI. HYDRAULIC FLUME DATA AND VELOCITY DISTRIBUTION CALCULATIONS USING THE PRANDTL TUBE WITHOUT SIMULATED RAINFALL ON A CONCRETE BED.

| Depth Above Bed, y | Point Velocity, v | Total Depth d | Mean Velocity, V | Shear Velocity $\sqrt{gdS}$ | $\frac{v - V}{\sqrt{gdS}}$ | $\frac{y}{d}$ | Friction Resistance f | $\frac{\frac{v}{V} - 1.0}{\sqrt{f}}$ |
|---|---|---|---|---|---|---|---|---|
| ft. | fps | ft. | fps | fps | | | | |
| 0.020 | 0.566 | 0.10 | 0.588 | 0.040 | -0.547 | 0.20 | 0.037 | -0.193 |
| 0.040 | 0.566 | | | | -0.547 | 0.40 | | -0.193 |
| 0.060 | 0.622 | | | | 0.850 | 0.60 | | 0.300 |
| 0.080 | 0.622 | | | | 0.850 | 0.80 | | 0.300 |
| 0.090 | 0.660 | | | | 1.797 | 0.90 | | 0.635 |
| 0.030 | 0.439 | 0.10 | 0.466 | 0.046 | -0.578 | 0.30 | 0.078 | -0.204 |
| 0.048 | 0.507 | | | | 0.898 | 0.48 | | 0.317 |
| 0.070 | 0.507 | | | | 0.898 | 0.70 | | 0.317 |
| 0.084 | 0.507 | | | | 0.898 | 0.84 | | 0.317 |
| 0.020 | 0.507 | 0.10 | 0.522 | 0.046 | -0.328 | 0.20 | 0.062 | -0.116 |
| 0.030 | 0.507 | | | | -0.328 | 0.30 | | -0.116 |
| 0.048 | 0.507 | | | | -0.328 | 0.48 | | -0.116 |
| 0.070 | 0.566 | | | | 0.953 | 0.70 | | 0.337 |
| 0.084 | 0.566 | | | | 0.953 | 0.84 | | 0.337 |
| 0.020 | 0.878 | 0.20 | 1.025 | 0.065 | -2.256 | 0.10 | 0.032 | -0.798 |
| 0.040 | 0.982 | | | | -0.660 | 0.20 | | -0.233 |
| 0.080 | 1.014 | | | | -0.169 | 0.40 | | -0.060 |
| 0.120 | 1.045 | | | | 0.307 | 0.60 | | 0.108 |
| 0.160 | 1.105 | | | | 1.227 | 0.80 | | 0.434 |
| 0.180 | 1.163 | | | | 2.117 | 0.90 | | 0.749 |

TABLE VI. (continued)

| Depth Above Bed, y | Point Velocity, v | Total Depth d | Mean Velocity, V | Shear Velocity $\sqrt{gdS}$ | $\frac{v - V}{\sqrt{gdS}}$ | $\frac{y}{d}$ | Friction Resistance f | $\frac{\frac{v}{V} - 1.0}{\sqrt{f}}$ |
|---|---|---|---|---|---|---|---|---|
| ft. | fps | ft. | fps | fps | | | | |
| 0.020 | 0.802 | 0.20 | 0.938 | 0.065 | -2.085 | 0.10 | 0.039 | -0.737 |
| 0.060 | 0.878 | | | | -0.919 | 0.30 | | -0.325 |
| 0.096 | 0.949 | | | | 0.171 | 0.48 | | 0.602 |
| 0.140 | 1.014 | | | | 1.168 | 0.70 | | 0.413 |
| 0.169 | 1.075 | | | | 2.104 | 0.84 | | 0.744 |
| 0.020 | 0.802 | 0.20 | 0.938 | 0.065 | -2.085 | 0.10 | 0.039 | -0.737 |
| 0.060 | 0.878 | | | | -0.919 | 0.30 | | -0.325 |
| 0.096 | 0.949 | | | | 0.171 | 0.48 | | 0.060 |
| 0.140 | 1.014 | | | | 1.168 | 0.70 | | 0.413 |
| 0.169 | 1.075 | | | | 2.104 | 0.84 | | 0.744 |
| 0.030 | 1.216 | 0.30 | 1.429 | 0.090 | -2.378 | 0.10 | 0.031 | -0.841 |
| 0.060 | 1.317 | | | | -1.250 | 0.20 | | -0.442 |
| 0.120 | 1.433 | | | | 0.046 | 0.40 | | 0.016 |
| 0.180 | 1.478 | | | | 0.549 | 0.60 | | 0.194 |
| 0.240 | 1.583 | | | | 1.722 | 0.80 | | 0.609 |
| 0.270 | 1.604 | | | | 1.957 | 0.90 | | 0.692 |

TABLE VI. (continued)

| Depth Above Bed, y | Point Velocity, v | Total Depth d | Mean Velocity, V | Shear Velocity $\sqrt{gdS}$ | $\frac{v - V}{\sqrt{gdS}}$ | $\frac{y}{d}$ | Friction Resistance f | $\frac{\frac{v}{V} - 1.0}{\sqrt{f}}$ |
|---|---|---|---|---|---|---|---|---|
| ft. | fps | ft. | fps | fps | | | | |
| 0.030 | 1.105 | 0.30 | 1.330 | 0.090 | -2.515 | 0.10 | 0.036 | -0.889 |
| 0.090 | 1.293 | | | | -0.414 | 0.30 | | -0.146 |
| 0.144 | 1.342 | | | | 0.134 | 0.48 | | 0.047 |
| 0.210 | 1.433 | | | | 1.150 | 0.70 | | 0.407 |
| 0.254 | 1.478 | | | | 1.653 | 0.84 | | 0.584 |
| 0.271 | 1.500 | | | | 1.899 | 0.90 | | 0.671 |
| 0.286 | 1.541 | | | | 2.357 | 0.95 | | 0.833 |
| 0.030 | 1.190 | 0.30 | 1.356 | 0.090 | -1.854 | 0.10 | 0.035 | -0.656 |
| 0.090 | 1.317 | | | | -0.435 | 0.30 | | -0.154 |
| 0.144 | 1.366 | | | | 0.112 | 0.48 | | 0.040 |
| 0.210 | 1.432 | | | | 0.850 | 0.70 | | 0.300 |
| 0.254 | 0.478 | | | | 1.364 | 0.84 | | 0.482 |
| 0.271 | 1.499 | | | | 1.598 | 0.90 | | 0.565 |
| 0.286 | 1.499 | | | | 1.598 | 0.95 | | 0.565 |
| 0.040 | 1.317 | 0.40 | 1.563 | 0.103 | -2.383 | 0.10 | 0.035 | -0.842 |
| 0.120 | 1.541 | | | | -0.215 | 0.30 | | -0.076 |
| 0.191 | 1.583 | | | | 0.191 | 0.48 | | 0.067 |
| 0.280 | 1.682 | | | | 1.149 | 0.70 | | 0.406 |
| 0.338 | 1.720 | | | | 1.517 | 0.84 | | 0.536 |
| 0.361 | 1.757 | | | | 1.875 | 0.90 | | 0.663 |
| 0.382 | 1.737 | | | | 1.681 | 0.95 | | 0.594 |

TABLE VI. (continued)

| Depth Above Bed, y ft. | Point Velocity, v fps | Total Depth d ft. | Mean Velocity, V fps | Shear Velocity $\sqrt{gdS}$ fps | $\frac{v - V}{\sqrt{gdS}}$ | $\frac{y}{d}$ | Friction Resistance f | $\frac{\frac{v}{V} - 1.0}{\sqrt{f}}$ |
|---|---|---|---|---|---|---|---|---|
| 0.040 | 1.366 | 0.40 | 1.547 | 0.103 | -1.750 | 0.10 | 0.036 | -0.619 |
| 0.120 | 1.499 | | | | -0.463 | 0.30 | | -0.164 |
| 0.191 | 1.562 | | | | 0.147 | 0.48 | | 0.052 |
| 0.280 | 1.624 | | | | 0.747 | 0.70 | | 0.264 |
| 0.338 | 1.682 | | | | 1.308 | 0.84 | | 0.462 |
| 0.361 | 1.720 | | | | 1.676 | 0.90 | | 0.592 |
| 0.050 | 1.604 | 0.50 | 1.844 | 0.127 | -1.894 | 0.10 | 0.039 | -0.670 |
| 0.100 | 1.720 | | | | -0.980 | 0.20 | | -0.346 |
| 0.200 | 1.864 | | | | 0.156 | 0.40 | | 0.055 |
| 0.300 | 1.915 | | | | 0.558 | 0.60 | | 0.197 |
| 0.400 | 1.996 | | | | 1.196 | 0.80 | | 0.423 |
| 0.450 | 2.030 | | | | 1.464 | 0.90 | | 0.518 |
| 0.050 | 1.604 | 0.50 | 1.810 | 0.127 | -1.629 | 0.10 | 0.039 | -0.576 |
| 0.150 | 1.757 | | | | -0.423 | 0.30 | | -0.150 |
| 0.239 | 1.828 | | | | 0.137 | 0.48 | | 0.048 |
| 0.350 | 1.931 | | | | 0.949 | 0.70 | | 0.336 |
| 0.422 | 1.965 | | | | 1.217 | 0.84 | | 0.430 |
| 0.451 | 1.965 | | | | 1.217 | 0.90 | | 0.430 |
| 0.477 | 1.980 | | | | 1.335 | 0.95 | | 0.472 |

TABLE VI. (continued)

| Depth Above Bed, y | Point Velocity, v | Total Depth d | Mean Velocity, V | Shear Velocity $\sqrt{gdS}$ | $\frac{v - V}{\sqrt{gdS}}$ | $\frac{y}{d}$ | Friction Resistance f | $\frac{\frac{v}{V} - 1.0}{\sqrt{f}}$ |
|---|---|---|---|---|---|---|---|---|
| ft. | fps | ft. | fps | fps | | | | |
| 0.050 | 1.478 | 0.50 | 1.734 | 0.127 | -2.015 | 0.10 | 0.043 | -0.713 |
| 0.150 | 1.673 | | | | -0.478 | 0.30 | | -0.169 |
| 0.239 | 1.774 | | | | 0.319 | 0.48 | | 0.113 |
| 0.350 | 1.880 | | | | 1.154 | 0.70 | | 0.408 |
| 0.422 | 1.913 | | | | 1.414 | 0.84 | | 0.500 |
| 0.451 | 1.930 | | | | 1.549 | 0.90 | | 0.547 |
| 0.477 | 1.913 | | | | 1.414 | 0.95 | | 0.500 |

TABLE VII. HYDRAULIC FLUME DATA AND VELOCITY DISTRIBUTION CALCULATIONS USING THE PRANDTL TUBE WITH SIMULATED RAINFALL ON A CONCRETE BED.

| Depth Above Bed, y | Point Velocity, v | Total Depth d | Mean Velocity, V | Shear Velocity $\sqrt{gdS}$ | $\frac{v - V}{\sqrt{gdS}}$ | $\frac{y}{d}$ | Friction Resistance f | $\frac{\frac{v}{V} - 1.0}{\sqrt{f}}$ |
|---|---|---|---|---|---|---|---|---|
| ft. | fps | ft. | fps | fps | | | | |
| 0.020 | 0.359 | 0.10 | 0.410 | 0.046 | -1.115 | 0.20 | 0.101 | -0.394 |
| 0.040 | 0.359 | | | | -1.115 | 0 40 | | -0.394 |
| 0.060 | 0.507 | | | | 2.097 | 0.60 | | 0.741 |
| 0.080 | 0.507 | | | | 2.097 | 0.80 | | 0.741 |
| 0.030 | 0.359 | 0.10 | 0.390 | 0.046 | -0.664 | 0.30 | 0.112 | -0.235 |
| 0.048 | 0.439 | | | | 1.072 | 0.48 | | 0.379 |
| 0.070 | 0.439 | | | | 1.072 | 0.70 | | 0.379 |
| 0.020 | 0.439 | 0.10 | 0.449 | 0.046 | -0.207 | 0.20 | 0.084 | -0.073 |
| 0.030 | 0.439 | | | | -0.207 | 0.30 | | -0.073 |
| 0.048 | 0.439 | | | | -0.207 | 0.48 | | -0.073 |
| 0.070 | 0.507 | | | | 1.269 | 0.70 | | 0.449 |
| 0.085 | 0.439 | | | | -0.207 | 0.84 | | -0.073 |
| 0.020 | 0.878 | 0.20 | 0.972 | 0.073 | -1.283 | 0.10 | 0.045 | -0.454 |
| 0.040 | 0.949 | | | | -0.312 | 0.20 | | -0.110 |
| 0.080 | 0.982 | | | | 0.140 | 0.40 | | 0.050 |
| 0.120 | 1.014 | | | | 0.578 | 0.60 | | 0.204 |
| 0.160 | 1.014 | | | | 0.578 | 0.80 | | 0.204 |
| 0.180 | 1.014 | | | | 0.578 | 0.90 | | 0.204 |

TABLE VII. (continued)

| Depth Above Bed, y | Point Velocity, v | Total Depth d | Mean Velocity, V | Shear Velocity $\sqrt{gdS}$ | $\frac{v - V}{\sqrt{gdS}}$ | $\frac{y}{d}$ | Friction Resistance f | $\frac{\frac{v}{V} - 1.0}{\sqrt{f}}$ |
|---|---|---|---|---|---|---|---|---|
| ft. | fps | ft. | fps | fps | | | | |
| 0.020 | 0.718 | 0.20 | 0.833 | 0.073 | -1.578 | 0.10 | 0.062 | -0.558 |
| 0.060 | 0.802 | | | | -0.429 | 0.30 | | -0.152 |
| 0.096 | 0.841 | | | | 0.105 | 0.48 | | 0.037 |
| 0.140 | 0.914 | | | | 1.104 | 0.70 | | 0.390 |
| 0.169 | 0.914 | | | | 1.104 | 0.84 | | 0.390 |
| 0.020 | 0.718 | 0.20 | 0.869 | 0.073 | -2.062 | 0.10 | 0.057 | -0.729 |
| 0.060 | 0.841 | | | | -0.379 | 0.30 | | -0.134 |
| 0.096 | 0.914 | | | | 0.620 | 0.48 | | 0.219 |
| 0.140 | 0.948 | | | | 1.086 | 0.70 | | 0.384 |
| 0.169 | 0.949 | | | | 1.099 | 0.84 | | 0.389 |
| 0.030 | 1.134 | 0.30 | 1.289 | 0.098 | -1.574 | 0.10 | 0.046 | -0.557 |
| 0.060 | 1.163 | | | | -1.279 | 0.20 | | -0.452 |
| 0.120 | 1.293 | | | | 0.044 | 0.40 | | 0.016 |
| 0.180 | 1.388 | | | | 1.011 | 0.60 | | 0.357 |
| 0.240 | 1.388 | | | | 1.011 | 0.80 | | 0.357 |
| 0.270 | 1.412 | | | | 1.255 | 0.90 | | 0.444 |

TABLE VII. (continued)

| Depth Above Bed, y | Point Velocity, v | Total Depth d | Mean Velocity, V | Shear Velocity $\sqrt{gdS}$ | $\frac{v - V}{\sqrt{gdS}}$ | $\frac{y}{d}$ | Friction Resistance f | $\frac{\frac{v}{V} - 1.0}{\sqrt{f}}$ |
|---|---|---|---|---|---|---|---|---|
| ft. | fps | ft. | fps | fps | | | | |
| 0.030 | 1.075 | 0.30 | 1.260 | 0.098 | -1.880 | 0.10 | 0.049 | -0.665 |
| 0.090 | 1.216 | | | | -0.444 | 0.30 | | -0.157 |
| 0.144 | 1.293 | | | | 0.339 | 0.48 | | 0.120 |
| 0.210 | 1.365 | | | | 1.072 | 0.70 | | 0.379 |
| 0.254 | 1.388 | | | | 1.306 | 0.84 | | 0.462 |
| 0.271 | 1.388 | | | | 1.306 | 0.90 | | 0.462 |
| 0.030 | 1.134 | 0.30 | 1.287 | 0.098 | -1.558 | 0.10 | 0.047 | -0.551 |
| 0.090 | 1.242 | | | | -0.459 | 0.30 | | -0.162 |
| 0.144 | 1.341 | | | | 0.549 | 0.48 | | 0.194 |
| 0.210 | 1.366 | | | | 0.803 | 0.70 | | 0.284 |
| 0.254 | 1.366 | | | | 0.803 | 0.84 | | 0.284 |
| 0.271 | 1.411 | | | | 1.261 | 0.90 | | 0.446 |
| 0.040 | 1.317 | 0.40 | 1.516 | 0.113 | -1.755 | 0.10 | 0.045 | -0.620 |
| 0.120 | 1.478 | | | | -0.335 | 0.30 | | -0.119 |
| 0.191 | 1.563 | | | | 0.414 | 0.48 | | 0.146 |
| 0.280 | 1.623 | | | | 0.943 | 0.70 | | 0.333 |
| 0.338 | 1.644 | | | | 1.128 | 0.84 | | 0.399 |
| 0.361 | 1.644 | | | | 1.128 | 0.90 | | 0.399 |

TABLE VII. (continued)

| Depth Above Bed, y | Point Velocity, v | Total Depth d | Mean Velocity, V | Shear Velocity $\sqrt{gdS}$ | $\frac{v - V}{\sqrt{gdS}}$ | $\frac{y}{d}$ | Friction Resistance f | $\frac{\frac{v}{V} - 1.0}{\sqrt{f}}$ |
|---|---|---|---|---|---|---|---|---|
| ft. | fps | ft. | fps | fps | | | | |
| 0.040 | 1.294 | 0.40 | 1.475 | 0.113 | -1.597 | 0.10 | 0.047 | -0.565 |
| 0.120 | 1.432 | | | | -0.381 | 0.30 | | -0.135 |
| 0.191 | 1.499 | | | | 0.210 | 0.48 | | 0.074 |
| 0.280 | 1.583 | | | | 0.950 | 0.70 | | 0.336 |
| 0.338 | 1.604 | | | | 1.135 | 0.84 | | 0.401 |
| 0.361 | 1.604 | | | | 1.135 | 0.90 | | 0.401 |
| 0.050 | 1.604 | 0.50 | 1.738 | 0.137 | -0.980 | 0.10 | 0.049 | -0.346 |
| 0.100 | 1.682 | | | | -0.409 | 0.20 | | -0.145 |
| 0.200 | 1.775 | | | | 0.272 | 0.40 | | 0.096 |
| 0.300 | 1.880 | | | | 1.041 | 0.60 | | 0.368 |
| 0.400 | 1.757 | | | | 0.140 | 0.80 | | 0.050 |
| 0.450 | 1.757 | | | | 0.140 | 0.90 | | 0.050 |
| 0.050 | 1.563 | 0.50 | 1.772 | 0.137 | -1.529 | 0.10 | 0.048 | -0.541 |
| 0.150 | 1.757 | | | | -0.109 | 0.30 | | -0.039 |
| 0.239 | 1.810 | | | | 0.279 | 0.48 | | 0.099 |
| 0.350 | 1.880 | | | | 0.792 | 0.70 | | 0.280 |
| 0.422 | 1.915 | | | | 1.048 | 0.84 | | 0.370 |
| 0.451 | 1.931 | | | | 1.165 | 0.90 | | 0.412 |
| 0.477 | 1.864 | | | | 0.674 | 0.95 | | 0.238 |

TABLE VII. (continued)

| Depth Above Bed, y | Point Velocity, v | Total Depth d | Mean Velocity, V | Shear Velocity $\sqrt{gdS}$ | $\frac{v - V}{\sqrt{gdS}}$ | $\frac{y}{d}$ | Friction Resistance f | $\frac{\frac{v}{V} - 1.0}{\sqrt{f}}$ |
|---|---|---|---|---|---|---|---|---|
| ft. | fps | ft. | fps | fps | | | | |
| 0.050 | 1.499 | 0.50 | 1.735 | 0.137 | -1.728 | 0.10 | 0.050 | -0.611 |
| 0.150 | 1.700 | | | | -0.257 | 0.30 | | -0.091 |
| 0.239 | 1.774 | | | | 0.285 | 0.48 | | 0.101 |
| 0.350 | 1.845 | | | | 0.805 | 0.70 | | 0.284 |
| 0.422 | 1.897 | | | | 1.185 | 0.84 | | 0.419 |
| 0.451 | 1.930 | | | | 1.427 | 0.90 | | 0.504 |
| 0.477 | 1.880 | | | | 1.061 | 0.95 | | 0.375 |

TABLE VIII. HYDRAULIC FLUME DATA AND VELOCITY DISTRIBUTION CALCULATIONS USING THE TOTAL HEAD PROBE WITHOUT SIMULATED RAINFALL ON A CONCRETE BED.

| Depth Above Bed, y | Point Velocity, v | Total Depth d | Mean Velocity, V | Shear Velocity $\sqrt{gdS}$ | $\frac{v - V}{\sqrt{gdS}}$ | $\frac{y}{d}$ | Friction Resistance f | $\frac{\frac{v}{V} - 1.0}{\sqrt{f}}$ |
|---|---|---|---|---|---|---|---|---|
| ft. | fps | ft. | fps | fps | | | | |
| 0.010 | 0.818 | 0.20 | 0.963 | 0.080 | -1.804 | 0.05 | 0.056 | -0.638 |
| 0.020 | 0.818 | | | | -1.804 | 0.10 | | -0.638 |
| 0.040 | 0.904 | | | | -0.732 | 0.20 | | -0.259 |
| 0.060 | 0.904 | | | | -0.732 | 0.30 | | -0.259 |
| 0.100 | 0.983 | | | | 0.253 | 0.50 | | 0.089 |
| 0.140 | 1.020 | | | | 0.714 | 0.70 | | 0.253 |
| 0.160 | 1.056 | | | | 1.163 | 0.80 | | 0.411 |
| 0.180 | 1.056 | | | | 1.163 | 0.90 | | 0.411 |
| 0.190 | 1.056 | | | | 1.163 | 0.95 | | 0.411 |
| 0.010 | 0.944 | 0.30 | 1.267 | 0.090 | -3.607 | 0.03 | 0.040 | -1.275 |
| 0.030 | 1.020 | | | | -2.758 | 0.10 | | -0.975 |
| 0.060 | 1.124 | | | | -1.596 | 0.20 | | -0.564 |
| 0.090 | 1.249 | | | | -0.200 | 0.30 | | -0.071 |
| 0.150 | 1.307 | | | | 0.449 | 0.50 | | 0.159 |
| 0.210 | 1.363 | | | | 1.074 | 0.70 | | 0.380 |
| 0.240 | 1.417 | | | | 1.678 | 0.80 | | 0.593 |
| 0.270 | 1.417 | | | | 1.678 | 0.90 | | 0.593 |
| 0.290 | 1.417 | | | | 1.678 | 0.97 | | 0.593 |

TABLE VIII. (continued)

| Depth Above Bed, y | Point Velocity, v | Total Depth d | Mean Velocity, V | Shear Velocity $\sqrt{gdS}$ | $\frac{v - V}{\sqrt{gdS}}$ | $\frac{y}{d}$ | Friction Resistance f | $\frac{\frac{v}{V} - 1.0}{\sqrt{f}}$ |
|---|---|---|---|---|---|---|---|---|
| ft. | fps | ft. | fps | fps | | | | |
| 0.010 | 1.124 | 0.40 | 1.564 | 0.103 | -4.256 | 0.03 | 0.035 | -1.504 |
| 0.040 | 1.307 | | | | -2.485 | 0.10 | | -0.879 |
| 0.080 | 1.417 | | | | -1.421 | 0.20 | | -0.502 |
| 0.120 | 1.363 | | | | -1.943 | 0.30 | | -0.687 |
| 0.200 | 1.590 | | | | 0.253 | 0.50 | | 0.089 |
| 0.280 | 1.636 | | | | 0.698 | 0.70 | | 0.247 |
| 0.320 | 1.636 | | | | 0.698 | 0.80 | | 0.247 |
| 0.360 | 1.680 | | | | 1.123 | 0.90 | | 0.397 |
| 0.380 | 1.869 | | | | 2.952 | 0.95 | | 1.044 |
| 0.390 | 1.966 | | | | 3.891 | 0.98 | | 1.376 |
| 0.010 | 0.944 | 0.50 | 1.747 | 0.127 | -6.331 | 0.02 | 0.042 | -2.238 |
| 0.050 | 1.335 | | | | -3.248 | 0.10 | | -1.148 |
| 0.100 | 1.518 | | | | -1.805 | 0.20 | | -0.638 |
| 0.150 | 1.703 | | | | -0.347 | 0.30 | | -0.123 |
| 0.250 | 1.849 | | | | 0.804 | 0.50 | | 0.284 |
| 0.350 | 1.966 | | | | 1.727 | 0.70 | | 0.611 |
| 0.400 | 1.984 | | | | 1.869 | 0.80 | | 0.661 |
| 0.450 | 2.004 | | | | 2.027 | 0.90 | | 0.717 |
| 0.480 | 2.004 | | | | 2.027 | 0.96 | | 0.717 |

TABLE IX. HYDRAULIC FLUME DATA AND VELOCITY DISTRIBUTION CALCULATIONS USING THE TOTAL HEAD PROBE WITH SIMULATED RAINFALL ON A CONCRETE BED.

| Depth Above Bed, y | Point Velocity, v | Total Depth d | Mean Velocity, V | Shear Velocity $\sqrt{gdS}$ | $\frac{v - V}{\sqrt{gdS}}$ | $\frac{y}{d}$ | Friction Resistance f | $\frac{v}{V} - 1.0$ / $\sqrt{f}$ |
|---|---|---|---|---|---|---|---|---|
| ft. | fps | ft. | fps | fps | | | | |
| 0.010 | 0.771 | 0.20 | 0.947 | 0.065 | -2.697 | 0.05 | 0.038 | -0.953 |
| 0.020 | 0.818 | | | | -1.976 | 0.10 | | -0.698 |
| 0.040 | 0.904 | | | | -0.656 | 0.20 | | -0.232 |
| 0.060 | 0.944 | | | | -0.042 | 0.30 | | -0.015 |
| 0.100 | 0.944 | | | | -0.042 | 0.50 | | -0.015 |
| 0.140 | 1.020 | | | | 1.124 | 0.70 | | 0.398 |
| 0.160 | 1.020 | | | | 1.124 | 0.80 | | 0.398 |
| 0.180 | 1.020 | | | | 1.124 | 0.90 | | 0.398 |
| 0.010 | 0.983 | 0.30 | 1.253 | 0.098 | -2.749 | 0.03 | 0.049 | -0.972 |
| 0.030 | 1.020 | | | | -2.372 | 0.10 | | -0.838 |
| 0.060 | 1.157 | | | | -0.978 | 0.20 | | -0.346 |
| 0.090 | 1.219 | | | | -0.347 | 0.30 | | -0.123 |
| 0.150 | 1.307 | | | | 0.549 | 0.50 | | 0.194 |
| 0.210 | 1.363 | | | | 1.119 | 0.70 | | 0.396 |
| 0.240 | 1.363 | | | | 1.119 | 0.80 | | 0.396 |
| 0.270 | 1.363 | | | | 1.119 | 0.90 | | 0.396 |

TABLE IX.. (continued)

| Depth Above Bed, y | Point Velocity, v | Total Depth d | Mean Velocity, V | Shear Velocity $\sqrt{gdS}$ | $\frac{v - V}{\sqrt{gdS}}$ | $\frac{y}{d}$ | Friction Resistance f | $\frac{\frac{v}{V} - 1.0}{\sqrt{f}}$ |
|---|---|---|---|---|---|---|---|---|
| ft. | fps | ft. | fps | fps | | | | |
| 0.010 | 1.157 | 0.40 | 1.599 | 0.113 | -3.899 | 0.03 | 0.040 | -1.378 |
| 0.040 | 1.335 | | | | -2.329 | 0.10 | | -0.824 |
| 0.080 | 1.468 | | | | -1.157 | 0.20 | | -0.409 |
| 0.120 | 1.518 | | | | -0.716 | 0.30 | | -0.253 |
| 0.200 | 1.659 | | | | 0.527 | 0.50 | | 0.186 |
| 0.280 | 1.613 | | | | 0.121 | 0.70 | | 0.043 |
| 0.320 | 1.680 | | | | 0.712 | 0.80 | | 0.252 |
| 0.360 | 1.889 | | | | 2.554 | 0.90 | | 0.903 |
| 0.380 | 1.849 | | | | 2.202 | 0.95 | | 0.778 |
| 0.010 | 1.020 | 0.50 | 1.759 | 0.137 | -5.409 | 0.02 | 0.048 | -1.921 |
| 0.050 | 1.468 | | | | -2.130 | 0.10 | | -0.753 |
| 0.100 | 1.590 | | | | -1.236 | 0.20 | | -0.437 |
| 0.150 | 1.659 | | | | -0.731 | 0.30 | | -0.259 |
| 0.250 | 1.849 | | | | 0.660 | 0.50 | | 0.233 |
| 0.350 | 1.947 | | | | 1.377 | 0.70 | | 0.487 |
| 0.400 | 1.966 | | | | 1.516 | 0.80 | | 0.536 |
| 0.450 | 1.966 | | | | 1.516 | 0.90 | | 0.536 |

TABLE X. HYDRAULIC FLUME DATA AND VELOCITY DISTRIBUTION CALCULATIONS USING THE PRANDTL TUBE WITHOUT SIMULATED RAINFALL ON A PLYWOOD BED.

| Depth Above Bed, y | Point Velocity, v | Total Depth d | Mean Velocity, V | Shear Velocity $\sqrt{gdS}$ | $\frac{v - V}{\sqrt{gdS}}$ | $\frac{y}{d}$ | Friction Resistance f | $\frac{\frac{v}{V} - 1.0}{\sqrt{f}}$ |
|---|---|---|---|---|---|---|---|---|
| ft. | fps | ft. | fps | fps | | | | |
| 0.020 | 1.190 | 0.20 | 1.459 | 0.080 | -3.352 | 0.10 | 0.024 | -1.185 |
| 0.040 | 1.342 | | | | -1.457 | 0.20 | | -0.515 |
| 0.060 | 1.412 | | | | -0.584 | 0.30 | | -0.206 |
| 0.100 | 1.522 | | | | 0.787 | 0.50 | | 0.278 |
| 0.140 | 1.563 | | | | 1.299 | 0.70 | | 0.459 |
| 0.160 | 1.624 | | | | 2.059 | 0.80 | | 0.728 |
| 0.180 | 1.663 | | | | 2.545 | 0.90 | | 0.900 |
| 0.020 | 1.604 | 0.30 | 1.873 | 0.098 | -2.743 | 0.07 | 0.022 | -0.970 |
| 0.030 | 1.623 | | | | -2.550 | 0.10 | | -0.901 |
| 0.060 | 1.720 | | | | -1.562 | 0.20 | | -0.552 |
| 0.090 | 1.811 | | | | -0.636 | 0.30 | | -0.225 |
| 0.150 | 1.931 | | | | 0.585 | 0.50 | | 0.207 |
| 0.210 | 1.981 | | | | 1.094 | 0.70 | | 0.387 |
| 0.240 | 2.028 | | | | 1.573 | 0.80 | | 0.556 |
| 0.270 | 2.060 | | | | 1.899 | 0.90 | | 0.671 |
| 0.290 | 2.060 | | | | 1.899 | 0.97 | | 0.671 |

TABLE X. (continued)

| Depth Above Bed, y | Point Velocity, v | Total Depth d | Mean Velocity, V | Shear Velocity $\sqrt{gdS}$ | $\frac{v - V}{\sqrt{gdS}}$ | $\frac{y}{d}$ | Friction Resistance f | $\frac{\frac{v}{V} - 1.0}{\sqrt{f}}$ |
|---|---|---|---|---|---|---|---|---|
| ft. | fps | ft. | fps | fps | | | | |
| 0.020 | 1.663 | 0.40 | 2.082 | 0.113 | -3.690 | 0.05 | 0.024 | -1.305 |
| 0.040 | 1.775 | | | | -2.702 | 0.10 | | -0.956 |
| 0.080 | 1.931 | | | | -1.327 | 0.20 | | -0.469 |
| 0.120 | 2.029 | | | | -0.464 | 0.30 | | -0.164 |
| 0.200 | 2.122 | | | | 0.356 | 0.50 | | 0.126 |
| 0.280 | 2.211 | | | | 1.141 | 0.70 | | 0.403 |
| 0.320 | 2.270 | | | | 1.661 | 0.80 | | 0.587 |
| 0.360 | 2.290 | | | | 1.837 | 0.90 | | 0.650 |
| 0.380 | 2.322 | | | | 2.119 | 0.95 | | 0.749 |

TABLE XI. HYDRAULIC FLUME DATA AND VELOCITY DISTRIBUTION CALCULATIONS USING THE PRANDTL TUBE WITH SIMULATED RAINFALL ON A PLYWOOD BED.

| Depth Above Bed, y | Point Velocity, v | Total Depth d | Mean Velocity, V | Shear Velocity $\sqrt{gdS}$ | $\frac{v - V}{\sqrt{gdS}}$ | $\frac{y}{d}$ | Friction Resistance f | $\frac{v}{V} - 1.0$ / $\sqrt{f}$ |
|---|---|---|---|---|---|---|---|---|
| ft. | fps | ft. | fps | fps | | | | |
| 0.020 | 1.134 | 0.215 | 1.466 | 0.083 | -3.989 | 0.093 | 0.026 | -1.410 |
| 0.040 | 1.342 | | | | -1.488 | 0.186 | | -0.526 |
| 0.060 | 1.412 | | | | -0.646 | 0.279 | | -0.228 |
| 0.100 | 1.522 | | | | 0.677 | 0.465 | | 0.239 |
| 0.140 | 1.563 | | | | 1.170 | 0.651 | | 0.414 |
| 0.160 | 1.624 | | | | 1.903 | 0.744 | | 0.673 |
| 0.180 | 1.663 | | | | 2.372 | 0.837 | | 0.839 |
| 0.020 | 1.522 | 0.310 | 1.795 | 0.100 | -2.735 | 0.065 | 0.025 | -0.967 |
| 0.030 | 1.541 | | | | 2.545 | 0.097 | | -0.900 |
| 0.060 | 1.682 | | | | -1.133 | 0.194 | | -0.401 |
| 0.090 | 1.739 | | | | -0.562 | 0.290 | | -0.199 |
| 0.150 | 1.811 | | | | 0.159 | 0.484 | | 0.056 |
| 0.210 | 1.915 | | | | 1.200 | 0.667 | | 0.424 |
| 0.240 | 1.948 | | | | 1.531 | 0.774 | | 0.541 |
| 0.270 | 1.948 | | | | 1.531 | 0.871 | | 0.541 |

TABLE XI. (continued)

| Depth Above Bed, y | Point Velocity, v | Total Depth d | Mean Velocity, V | Shear Velocity $\sqrt{gdS}$ | $\frac{v - V}{\sqrt{gdS}}$ | $\frac{y}{d}$ | Friction Resistance f | $\frac{v}{V} - 1.0$ / $\sqrt{f}$ |
|---|---|---|---|---|---|---|---|---|
| ft. | fps | ft. | fps | fps | | | | |
| 0.020 | 1.624 | 0.405 | 2.068 | 0.114 | -3.893 | 0.049 | 0.024 | -1.377 |
| 0.040 | 1.793 | | | | -2.413 | 0.099 | | -0.853 |
| 0.080 | 1.931 | | | | -1.204 | 0.198 | | -0.426 |
| 0.120 | 2.012 | | | | -0.495 | 0.296 | | -0.175 |
| 0.200 | 2.122 | | | | 0.469 | 0.494 | | 0.166 |
| 0.280 | 2.211 | | | | 1.249 | 0.691 | | 0.441 |
| 0.320 | 2.240 | | | | 1.503 | 0.790 | | 0.531 |
| 0.360 | 2.270 | | | | 1.766 | 0.889 | | 0.624 |
| 0.380 | 2.270 | | | | 1.766 | 0.938 | | 0.624 |

TABLE XII. HYDRAULIC FLUME DATA AND VELOCITY DISTRIBUTION CALCULATIONS USING THE PITOT-STATIC TUBE WITHOUT SIMULATED RAINFALL ON A PLYWOOD BED.

| Depth Above Bed, y | Point Velocity, v | Total Depth d | Mean Velocity, V | Shear Velocity $\sqrt{gdS}$ | $\frac{v - V}{\sqrt{gdS}}$ | $\frac{y}{d}$ | Friction Resistance f | $\frac{v}{V} - 1.0$ / $\sqrt{f}$ |
|---|---|---|---|---|---|---|---|---|
| ft. | fps | ft. | fps | fps | | | | |
| 0.020 | 1.293 | 0.20 | 1.467 | 0.080 | -2.175 | 0.10 | 0.024 | -0.769 |
| 0.040 | 1.388 | | | | -0.991 | 0.20 | | -0.350 |
| 0.060 | 1.412 | | | | -0.691 | 0.30 | | -0.244 |
| 0.100 | 1.500 | | | | 0.406 | 0.50 | | 0.143 |
| 0.140 | 1.563 | | | | 1.191 | 0.70 | | 0.421 |
| 0.160 | 1.584 | | | | 1.453 | 0.80 | | 0.514 |
| 0.180 | 1.604 | | | | 1.702 | 0.90 | | 0.602 |
| 0.020 | 1.644 | 0.30 | 1.917 | 0.098 | -2.783 | 0.07 | 0.021 | -0.984 |
| 0.030 | 1.682 | | | | -2.397 | 0.10 | | -0.847 |
| 0.060 | 1.757 | | | | -1.633 | 0.20 | | -0.577 |
| 0.090 | 1.864 | | | | -0.544 | 0.30 | | -0.192 |
| 0.150 | 1.964 | | | | 0.474 | 0.50 | | 0.168 |
| 0.210 | 2.045 | | | | 1.299 | 0.70 | | 0.459 |
| 0.240 | 2.060 | | | | 1.451 | 0.80 | | 0.513 |
| 0.270 | 2.076 | | | | 1.614 | 0.90 | | 0.571 |
| 0.290 | 2.122 | | | | 2.082 | 0.97 | | 0.736 |

TABLE XI.. (continued)

| Depth Above Bed, y | Point Velocity, v | Total Depth d | Mean Velocity, V | Shear Velocity $\sqrt{gdS}$ | $\frac{v - V}{\sqrt{gdS}}$ | $\frac{y}{d}$ | Friction Resistance f | $\frac{\frac{v}{V} - 1.0}{\sqrt{f}}$ |
|---|---|---|---|---|---|---|---|---|
| ft. | fps | ft. | fps | fps | | | | |
| 0.010 | 1.644 | 0.40 | 2.109 | 0.113 | -4.100 | 0.03 | 0.023 | -1.450 |
| 0.040 | 1.829 | | | | -2.469 | 0.10 | | -0.873 |
| 0.080 | 1.948 | | | | -1.420 | 0.20 | | -0.502 |
| 0.120 | 2.076 | | | | -0.292 | 0.30 | | -0.103 |
| 0.200 | 2.137 | | | | 0.246 | 0.50 | | 0.087 |
| 0.280 | 2.240 | | | | 1.154 | 0.70 | | 0.408 |
| 0.320 | 2.268 | | | | 1.401 | 0.80 | | 0.495 |
| 0.360 | 2.297 | | | | 1.656 | 0.90 | | 0.586 |
| 0.380 | 2.310 | | | | 1.771 | 0.95 | | 0.626 |

TABLE XIII. HYDRAULIC FLUME DATA AND VELOCITY DISTRIBUTION CALCULATIONS USING THE PITOT-STATIC TUBE WITH SIMULATED RAINFALL ON A PLYWOOD BED.

| Depth Above Bed, y | Point Velocity, v | Total Depth d | Mean Velocity, V | Shear Velocity $\sqrt{gdS}$ | $\frac{v - V}{\sqrt{gdS}}$ | $\frac{y}{d}$ | Friction Resistance f | $\frac{\frac{v}{V} - 1.0}{\sqrt{f}}$ |
|---|---|---|---|---|---|---|---|---|
| ft. | fps | ft. | fps | fps | | | | |
| 0.020 | 1.190 | 0.215 | 1.375 | 0.083 | -2.225 | 0.093 | 0.029 | -0.787 |
| 0.040 | 1.268 | | | | -1.287 | 0.186 | | -0.455 |
| 0.060 | 1.318 | | | | -0.686 | 0.279 | | -0.242 |
| 0.100 | 1.412 | | | | 0.445 | 0.465 | | 0.157 |
| 0.140 | 1.479 | | | | 1.250 | 0.651 | | 0.442 |
| 0.160 | 1.479 | | | | 1.250 | 0.744 | | 0.442 |
| 0.180 | 1.479 | | | | 1.250 | 0.837 | | 0.442 |
| 0.020 | 1.563 | 0.310 | 1.820 | 0.100 | -2.576 | 0.064 | 0.024 | -0.911 |
| 0.030 | 1.563 | | | | -2.576 | 0.097 | | -0.911 |
| 0.060 | 1.663 | | | | -1.574 | 0.194 | | -0.557 |
| 0.090 | 1.757 | | | | -0.633 | 0.290 | | -0.224 |
| 0.150 | 1.864 | | | | 0.438 | 0.484 | | 0.155 |
| 0.210 | 1.948 | | | | 1.279 | 0.677 | | 0.452 |
| 0.240 | 1.964 | | | | 1.439 | 0.774 | | 0.509 |
| 0.270 | 1.981 | | | | 1.610 | 0.871 | | 0.569 |

TABLE XIII. (continued)

| Depth Above Bed, y | Point Velocity, v | Total Depth d | Mean Velocity, V | Shear Velocity $\sqrt{gdS}$ | $\frac{v - V}{\sqrt{gdS}}$ | $\frac{y}{d}$ | Friction Resistance f | $\frac{\frac{v}{V} - 1.0}{\sqrt{f}}$ |
|---|---|---|---|---|---|---|---|---|
| ft. | fps | ft. | fps | fps | | | | |
| 0.010 | 1.644 | 0.405 | 2.115 | 0.114 | -4.126 | 0.025 | 0.023 | -1.459 |
| 0.040 | 1.864 | | | | -2.199 | 0.099 | | -0.777 |
| 0.080 | 1.948 | | | | -1.463 | 0.198 | | -0.517 |
| 0.120 | 2.060 | | | | -0.482 | 0.296 | | -0.170 |
| 0.200 | 2.152 | | | | 0.324 | 0.494 | | 0.115 |
| 0.280 | 2.254 | | | | 1.218 | 0.691 | | 0.431 |
| 0.320 | 2.283 | | | | 1.472 | 0.790 | | 0.520 |
| 0.360 | 2.297 | | | | 1.594 | 0.889 | | 0.564 |
| 0.380 | 2.283 | | | | 1.472 | 0.938 | | 0.520 |

TABLE XIV . HYDRAULIC FLUME DATA AND VELOCITY DISTRIBUTION CALCULATIONS OBTAINED FROM SMERDON'S DOCTORAL DISSERTATION USING A DARCY TUBE. TESTS RUN OVER SEVERAL MISSOURI SOILS.

| Depth Above Bed, y | Point Velocity, v | Total Depth d | Mean Velocity, V | Shear Velocity $\sqrt{gdS}$ | $\frac{v - V}{\sqrt{gdS}}$ | $\frac{y}{d}$ | Friction Resistance f | $\frac{\frac{v}{V} - 1.0}{\sqrt{f}}$ |
|---|---|---|---|---|---|---|---|---|
| ft. | fps | ft. | fps | fps | | | | |
| 0.02 | 1.210 | 0.146 | 1.405 | 0.097 | -2.012 | 0.137 | 0.038 | -0.711 |
| 0.04 | 1.290 | | | | -1.187 | 0.274 | | -0.420 |
| 0.06 | 1.430 | | | | 0.258 | 0.411 | | 0.091 |
| 0.11 | 1.570 | | | | 1.702 | 0.753 | | 0.602 |
| 0.14 | 1.640 | | | | 2.425 | 0.959 | | 0.857 |
| 0.02 | 0.970 | 0.304 | 1.231 | 0.140 | -1.864 | 0.066 | 0.103 | -0.659 |
| 0.04 | 1.020 | | | | -1.507 | 0.132 | | -0.532 |
| 0.06 | 1.100 | | | | -0.935 | 0.197 | | -0.331 |
| 0.11 | 1.170 | | | | -0.434 | 0.362 | | -0.154 |
| 0.21 | 1.350 | | | | 0.853 | 0.691 | | 0.301 |
| 0.31 | 1.460 | | | | 1.639 | 1.020 | | 0.580 |
| 0.02 | 0.980 | 0.142 | 1.142 | 0.096 | -1.693 | 0.141 | 0.056 | -0.598 |
| 0.04 | 1.070 | | | | -0.751 | 0.282 | | -0.266 |
| 0.06 | 1.130 | | | | -0.123 | 0.423 | | -0.044 |
| 0.11 | 1.300 | | | | 1.655 | 0.775 | | 0.585 |
| 0.15 | 1.370 | | | | 2.387 | 1.056 | | 0.844 |

TABLE XIV. (continued)

| Depth Above Bed, y | Point Velocity, v | Total Depth d | Mean Velocity, V | Shear Velocity $\sqrt{gdS}$ | $\frac{v - V}{\sqrt{gdS}}$ | $\frac{y}{d}$ | Friction Resistance f | $\frac{\frac{v}{V} - 1.0}{\sqrt{f}}$ |
|---|---|---|---|---|---|---|---|---|
| ft. | fps | ft. | fps | fps | | | | |
| 0.02 | 0.730 | 0.225 | 1.250 | 0.120 | -4.322 | 0.089 | 0.074 | -1.528 |
| 0.04 | 1.150 | | | | -0.831 | 0.178 | | -0.294 |
| 0.06 | 1.160 | | | | -0.748 | 0.267 | | -0.264 |
| 0.11 | 1.350 | | | | 0.831 | 0.489 | | 0.294 |
| 0.21 | 1.500 | | | | 2.078 | 0.933 | | 0.735 |
| 0.23 | 1.540 | | | | 2.410 | 1.022 | | 0.852 |
| 0.02 | 1.210 | 0.485 | 1.746 | 0.177 | -3.035 | 0.041 | 0.082 | -1.073 |
| 0.04 | 1.240 | | | | -2.866 | 0.082 | | -1.013 |
| 0.06 | 1.330 | | | | -2.356 | 0.124 | | -0.833 |
| 0.11 | 1.570 | | | | -0.998 | 0.227 | | -0.353 |
| 0.21 | 1.770 | | | | 0.135 | 0.433 | | 0.048 |
| 0.31 | 1.910 | | | | 0.927 | 0.639 | | 0.328 |
| 0.41 | 2.050 | | | | 1.720 | 0.845 | | 0.608 |
| 0.46 | 2.060 | | | | 1.776 | 0.948 | | 0.628 |

TABLE XIV. (continued)

| Depth Above Bed, y | Point Velocity, v | Total Depth d | Mean Velocity, V | Shear Velocity $\sqrt{gdS}$ | $\frac{v - V}{\sqrt{gdS}}$ | $\frac{y}{d}$ | Friction Resistance f | $\frac{\frac{v}{V} - 1.0}{\sqrt{f}}$ |
|---|---|---|---|---|---|---|---|---|
| ft. | fps | ft, | fps | fps | | | | |
| 0.02 | 1.300 | 0.710 | 2.203 | 0.214 | -4.225 | 0.028 | 0.075 | -1.494 |
| 0.04 | 1.470 | | | | -3.430 | 0.056 | | -1.213 |
| 0.06 | 1.620 | | | | -2.728 | 0.085 | | -0.964 |
| 0.11 | 1.800 | | | | -1.886 | 0.155 | | -0.667 |
| 0.21 | 2.020 | | | | -0.856 | 0.296 | | -0.303 |
| 0.31 | 2.300 | | | | 0.454 | 0.437 | | 0.160 |
| 0.41 | 2.400 | | | | 0.922 | 0.577 | | 0.326 |
| 0.51 | 2.460 | | | | 1.202 | 0.718 | | 0.425 |
| 0.61 | 2.580 | | | | 1.764 | 0.859 | | 0.624 |
| 0.71 | 2.600 | | | | 1.857 | 1.000 | | 0.657 |
| 0.03 | 1.400 | 0.262 | 1.553 | 0.130 | -1.180 | 0.115 | 0.056 | -0.417 |
| 0.05 | 1.410 | | | | -1.103 | 0.191 | | -0.390 |
| 0.07 | 1.480 | | | | -0.563 | 0.267 | | -0.199 |
| 0.12 | 1.560 | | | | 0.053 | 0.458 | | 0.019 |
| 0.22 | 1.730 | | | | 1.362 | 0.840 | | 0.482 |
| 0.02 | 1.560 | 0.193 | 1.745 | 0.111 | -1.664 | 0.104 | 0.033 | -0.588 |
| 0.04 | 1.570 | | | | -1.574 | 0.207 | | -0.556 |
| 0.06 | 1.690 | | | | -0.427 | 0.311 | | -0.176 |
| 0.11 | 1.780 | | | | 0.311 | 0.570 | | 0.110 |
| 0.20 | 2.020 | | | | 2.464 | 1.036 | | 0.871 |

TABLE XIV . (continued)

| Depth Above Bed, y | Point Velocity, v | Total Depth d | Mean Velocity, V | Shear Velocity $\sqrt{gdS}$ | $\frac{v - V}{\sqrt{gdS}}$ | $\frac{y}{d}$ | Friction Resistance f | $\frac{\frac{v}{V} - 1.0}{\sqrt{f}}$ |
|---|---|---|---|---|---|---|---|---|
| ft. | fps | ft. | fps | fps | | | | |
| 0.02 | 1.030 | 0.288 | 1.396 | 0.136 | -2.692 | 0.069 | 0.076 | -0.952 |
| 0.04 | 1.100 | | | | -2.178 | 0.139 | | -0.770 |
| 0.06 | 1.160 | | | | -1.737 | 0.208 | | -0.614 |
| 0.11 | 1.320 | | | | -0.561 | 0.382 | | -0.199 |
| 0.21 | 1.610 | | | | 1.569 | 0.729 | | 0.555 |
| 0.27 | 1.730 | | | | 2.450 | 0.938 | | 0.866 |
| 0.02 | 1.100 | 0.440 | 1.638 | 0.168 | -3.197 | 0.045 | 0.084 | -1.130 |
| 0.04 | 1.190 | | | | -2.662 | 0.091 | | -0.941 |
| 0.06 | 1.350 | | | | -1.711 | 0.136 | | 0.605 |
| 0.11 | 1.530 | | | | -0.641 | 0.250 | | -0.227 |
| 0.21 | 1.720 | | | | 0.488 | 0.477 | | 0.173 |
| 0.31 | 1.830 | | | | 1.142 | 0.705 | | 0.404 |

TABLE XV. ANALYSIS OF VARIANCE RESULTS COMPARING RAINFALL AND NO RAINFALL FOR THE PRANDTL VELOCITY SENSING PROBE AND CONCRETE BED DATA.

| Source | df[+] | SS[++] | MS[+++] | F[++++] |
|---|---|---|---|---|
| Total | 160 | 212.91962 | | |
| Regression (1) | 1 | 186.60756 | 186.60756 | 1127.67*** |
| Residual (1) | 159 | 26.31206 | 0.16548 | |
| Additional due to second Reg. | 2 | 3.92083 | 1.96042 | 13.75** |
| Residual (2) | 157 | 22.39123 | 0.14262 | |

TABLE XVI. ANALYSIS OF VARIANCE RESULTS COMPARING RAINFALL AND NO RAINFALL FOR THE TOTAL HEAD VELOCITY SENSING PROBE AND CONCRETE BED DATA.

| Source | df | SS | MS | F |
|---|---|---|---|---|
| Total | 69 | 277.85539 | | |
| Regression (1) | 1 | 250.95158 | 250.95158 | 634.29*** |
| Residual (1) | 68 | 26.90381 | 0.39564 | |
| Additional due to second Reg. | 2 | 1.30167 | 0.65083 | 1.68 |
| Residual (2) | 66 | 25.60214 | 0.38791 | |

[+]df = degrees of freedom
[++]SS = sum of the squares
[+++]MS = mean square
[++++]F = statistic test for difference

** statistically significant at the 0.01 level
*** statistically significant at the 0.001 level

TABLE XVII. ANALYSIS OF VARIANCE RESULTS COMPARING RAINFALL AND NO RAINFALL FOR THE PRANDTL VELOCITY SENSING PROBE AND PLYWOOD BED DATA.

| Source | df | SS | MS | F |
|---|---|---|---|---|
| Total | 48 | 173.71527 | | |
| Regression (1) | 1 | 168.06453 | 168.06453 | 1397.97*** |
| Residual (1) | 47 | 5.65074 | 0.12022 | |
| Additional due to second Reg. | 2 | 0.01057 | 0.00528 | 0.42 |
| Residual (2) | 45 | 5.64017 | 0.12533 | |

TABLE XVIII. ANALYSIS OF VARIANCE RESULTS COMPARING RAINFALL AND NO RAINFALL FOR THE PITOT-STATIC VELOCITY SENSING PROBE AND PLYWOOD BED DATA.

| Source | df | SS | MS | F |
|---|---|---|---|---|
| Total | 48 | 140.91222 | | |
| Regression (1) | 1 | 138.13469 | 138.13469 | 2337.70*** |
| Residual (1) | 47 | 2.77753 | 0.05909 | |
| Additional due to second Reg. | 2 | 0.03728 | 0.01864 | 0.30 |
| Residual (2) | 45 | 2.74025 | 0.06089 | |

TABLE XIX. ANALYSIS OF VARIANCE RESULTS COMPARING BED DATA FOR THE PRANDTL VELOCITY SENSING PROBE WITHOUT RAINFALL.

| Source | df | SS | MS | F |
|---|---|---|---|---|
| Total | 107 | 225.42232 | | |
| Regression (1) | 1 | 211.85163 | 211 85163 | 1654.83*** |
| Residual (1) | 106 | 13.57069 | 0.12802 | |
| Additional due to second Reg. | 2 | 2.20445 | 1.10222 | 10.09** |
| Residual (2) | 104 | 11.36624 | 0.10929 | |

TABLE XX. ANALYSIS OF VARIANCE RESULTS COMPARING BED DATA FOR THE PRANDTL VELOCITY SENSING PROBE WITH RAINFALL.

| Source | df | SS | MS | F |
|---|---|---|---|---|
| Total | 101 | 165.13244 | | |
| Regression (1) | 1 | 140.94216 | 140.94216 | 582.65*** |
| Residual (1) | 100 | 24.19028 | 0.24190 | |
| Additional due to second Reg. | 2 | 7.52512 | 3.76256 | 22.13** |
| Residual (2) | 98 | 16.66516 | 0.17005 | |

TABLE XXI. ANALYSIS OF VARIANCE RESULTS COMPARING THE PRANDTL AND THE TOTAL HEAD VELOCITY SENSING PROBES FOR THE CONCRETE BED DATA WITHOUT RAINFALL.

| Source | df | SS | MS | F |
|---|---|---|---|---|
| Total | 119 | 309.46516 | | |
| Regression (1) | 1 | 280.97689 | 280.97689 | 1163.85*** |
| Residual (1) | 118 | 28.48827 | 0.24142 | |
| Additional due to second Reg. | 2 | 0.38914 | 0.19457 | 0.24 |
| Residual (2) | 116 | 28.09913 | 0.24223 | |

TABLE XXII. ANALYSIS OF VARIANCE RESULTS COMPARING THE PRANDTL AND THE PITOT-STATIC VELOCITY SENSING PROBES FOR THE PLYWOOD BED DATA WITHOUT RAINFALL.

| Source | df | SS | MS | F |
|---|---|---|---|---|
| Total | 49 | 164.14052 | | |
| Regression | 1 | 159.27481 | 159.27481 | 1571.38*** |
| Residual (1) | 48 | 4.86571 | 0.10136 | |
| Additional due to second Reg. | 2 | 1.05139 | 0.52569 | 6.34** |
| Residual (2) | 46 | 3.81432 | 0.08292 | |

TABLE XXIII. ANALYSIS OF VARIANCE RESULTS COMPARING A DARCY AND THE PRANDTL VELOCITY SENSING PROBES FOR THE SOIL BED AND A CONCRETE BED DATA WITHOUT RAINFALL.

| Source | df | SS | MS | F |
|---|---|---|---|---|
| Total | 144 | 353.20184 | | |
| Regression (1) | 1 | 292.48847 | 292.48847 | 688.47*** |
| Residual (1) | 143 | 60.75337 | 0.42484 | |
| Additional due to second Reg. | 2 | 38.03614 | 19.01807 | 118.04** |
| Residual (2) | 141 | 22.71723 | 0.16111 | |

TABLE XXIV. ANALYSIS OF VARIANCE RESULTS COMPARING A DARCY AND THE PRANDTL VELOCITY SENSING PROBES FOR THE SOIL BED AND A PLYWOOD BED DATA WITHOUT RAINFALL.

| Source | df | SS | MS | F |
|---|---|---|---|---|
| Total | 88 | 294.01456 | | |
| Regression (1) | 1 | 276.98465 | 276.98465 | 1382.50*** |
| Residual (1) | 87 | 17.02991 | 0.20035 | |
| Additional due to second Reg. | 2 | 0.90090 | 0.45045 | 2.37 |
| Residual (2) | 85 | 16.12901 | 0.18975 | |

TABLE XXV. GROUP TOTALS USED IN STATISTICAL ANALYSIS OF VARIANCE.

| Group* | 1 | 2 | 3 | 4 | 5 | 6 | 7 | 8 | 9 |
|---|---|---|---|---|---|---|---|---|---|
| N | 83 | 78 | 37 | 33 | 25 | 24 | 25 | 24 | 62 |
| $\Sigma Y$** | 27.164 | 16.678 | -5.988 | -11.001 | -0.212 | -3.811 | -1.597 | -4.786 | -23.909 |
| $\Sigma Y^2$ | 142.381 | 82.478 | 170.821 | 111.157 | 89.768 | 84.278 | 74.438 | 67.305 | 210.934 |
| $\Sigma X$*** | -28.619 | -28.438 | -17.449 | -17.383 | -10.975 | -11.343 | -11.276 | -11.644 | -33.234 |
| $\Sigma X^2$ | 18.383 | 18.324 | 16.882 | 16.880 | 8.741 | 9.085 | 9.615 | 9.962 | 28.626 |
| $\Sigma XY$ | 23.195 | 16.819 | 38.938 | 33.726 | 18.606 | 19.107 | 18.891 | 19.070 | 57.895 |
| SSE**** | 8.977 | 13.414 | 19.122 | 6.480 | 2.389 | 3.251 | 1.425 | 1.315 | 13.740 |

* Group notations are given in Table V

** $Y = \frac{v - V}{gdS}$

*** $X = \log_{10} \frac{y}{d}$

**** SSE = sum of the squares of the deviations from the regression